

Experimental Physiology – Lecture

Sharpey-Schafer Lecture Gas channels

Walter F. Boron

Department of Physiology and Biophysics, Case Western Reserve University School of Medicine, 10900 Euclid Avenue, Cleveland, OH 44106-4970, USA

The traditional dogma has been that all gases diffuse through all membranes simply by dissolving in the lipid phase of the membrane. Although this mechanism may explain how most gases move through most membranes, it is now clear that some membranes have no demonstrable gas permeability, and that at least two families of membrane proteins, the aquaporins (AQPs) and the Rhesus (Rh) proteins, can each serve as pathways for the diffusion of both CO₂ and NH₃. The knockout of RhCG in the renal collecting duct leads to the predicted consequences in acid–base physiology, providing a clear-cut role for at least one gas channel in the normal physiology of mammals. In our laboratory, we have found that surface-pH (pH_s) transients provide a sensitive approach for detecting CO₂ and NH₃ movement across the cell membranes of *Xenopus* oocytes. Using this approach, we have found that each tested AQP and Rh protein has its own characteristic CO₂/NH₃ permeability ratio, which provides the first demonstration of gas selectivity by a channel. Our preliminary AQP1 data suggest that all the NH₃ and less than half of the CO₂ move along with H₂O through the four monomeric aquapores. The majority of CO₂ takes an alternative route through AQP1, possibly the central pore at the four-fold axis of symmetry. Preliminary data with two Rh proteins, bacterial AmtB and human erythroid RhAG, suggest a similar story, with all the NH₃ moving through the three monomeric NH₃ pores and the CO₂ taking a separate route, perhaps the central pore at the three-fold axis of symmetry. The movement of different gases via different pathways is likely to underlie the gas selectivity that these channels exhibit.

(Received 1 September 2010; accepted after revision 10 September 2010; first published online 17 September 2010)

Corresponding author W. F. Boron: Department of Physiology and Biophysics, Case Western Reserve University School of Medicine, 10900 Euclid Avenue, Cleveland, OH 44106-4970, USA. Email: walter.boron@case.edu

Preface

This lecture honours Sir Edward Albert Sharpey-Schafer (1850–1935) and his grandson, Professor E. P. Sharpey-Schafer (1908–1963). The younger Sharpey-Schafer made important contributions to respiratory and cardiovascular physiology as a professor of medicine at St Thomas' Hospital in London (Anon, 1963).

The elder Sharpey-Schafer, working in London and Edinburgh, was a pioneer in the field of endocrinology and a major figure in the public service of the discipline of physiology (Hill, 1935). He made the pioneering discovery that a 'suprarenal extract' (i.e. predominantly adrenaline) increases blood pressure (Oliver & Schafer, 1895). He coined or popularized the terms 'endocrine',

'autocoid' and 'insuline' (from the Latin *insula* = island); the last, after hypothesizing that the substance that regulates blood glucose emanates from the islets of Langerhans. Sharpey-Schafer's closest link to the subject of my lecture was his work in the field of ventilation, including the introduction of the 'Schafer' method of artificial respiration, a procedure in which one straddles at the hips a patient in the prone position, and then periodically applies pressure with both hands on the back over the lower ribs.

As a distinguished servant in the cause of physiology, Sir Edward A. Sharpey-Schafer was a founding member of the Physiological Society (1876), the editor of *Advanced Textbook of Physiology* (1898–99) and the founder and lead editor of *The Quarterly Journal of Experimental Physiology* (1908), the predecessor to the present journal, the first editorial board of which also included Gotch, Halliburton, Sherrington, Starling and Waller.

This lecture was given at the Main meeting of the Physiological Society at the University of Cambridge on July 14, 2008.

Introduction: Overton's rule

The work of Overton. Over a century ago, Overton (Overton, 1897) performed a classic study on the algae *Spirogyra* in which he assessed the uptake of NH_3 and various amines by monitoring the precipitation that occurred as the amines combined with naturally occurring tannins. He found that extracellular acidification, which converts NH_3 to NH_4^+ and likewise converts primary, secondary and tertiary amines to their protonated/charged counterparts, reduces tannin precipitation. However, extracellular acidification had no effect in the case of

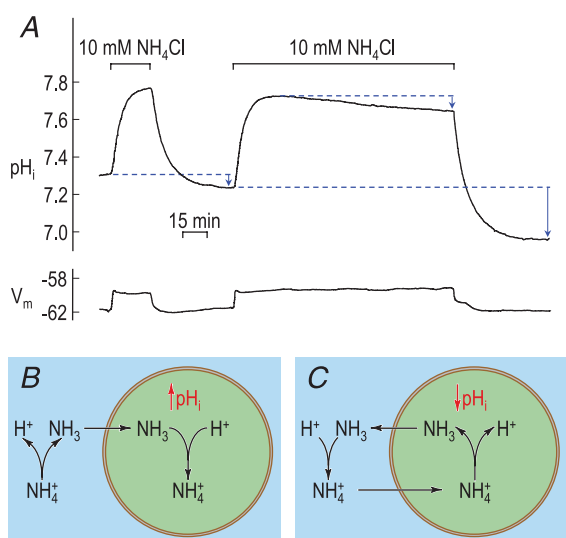


Figure 1. Effect of extracellular $\text{NH}_3/\text{NH}_4^+$ on intracellular pH (pH_i) of a squid giant axon, showing data (A), model of alkalinizing phase (B) and model of acidification during plateau phase (C)

Throughout the experiment in A, artificial seawater (ASW) with an extracellular pH of 7.70 flowed past a cannulated axon, which was suspended in a chamber of small volume. Intracellular pH and membrane potential (V_m) were monitored with glass microelectrodes. At the indicated times, the ASW was switched to one augmented with 10 mM NH_4Cl . Data are from Boron & De Weer (1976b). B shows that the influx of NH_3 leads to the consumption of intracellular H^+ and thus a rise in pH_i . This process accounts for the rising phase of pH_i during the two $\text{NH}_3/\text{NH}_4^+$ exposures in A. The influx of NH_3 in B leads to the dissociation of NH_4^+ near the extracellular surface of the membrane. In the bulk (i.e. flowing) ASW, the $\text{NH}_3/\text{NH}_4^+$ buffer was in equilibrium ($\text{NH}_3 + \text{H}^+ \rightleftharpoons \text{NH}_4^+$). C shows the system after NH_3 has equilibrated across the cell membrane; this equilibration corresponds to the peak pH_i during the second $\text{NH}_3/\text{NH}_4^+$ pulse in A. After this equilibration, pH_i is dominated by the influx of NH_4^+ ; this NH_4^+ influx had been occurring since the beginning of the $\text{NH}_3/\text{NH}_4^+$ exposure but its effect on pH_i had been overwhelmed by the influx of NH_3 . Now, during the plateau phase, the influx of NH_4^+ leads to a net dissociation of NH_4^+ in the cytosol. This process accounts for the plateau-phase acidification (i.e. falling phase of pH_i) during the second $\text{NH}_3/\text{NH}_4^+$ exposure in A. At the same time, the accumulation of NH_3 inside the cell now leads to the net efflux of NH_3 , some of which consumes H^+ on the outer surface of the cell, creating more NH_4^+ (the $\text{NH}_3/\text{NH}_4^+$ shuttle). Because the cell accumulated NH_4^+ during the $\text{NH}_3/\text{NH}_4^+$ exposure, the removal of extracellular $\text{NH}_3/\text{NH}_4^+$ leads to a pH_i undershoot.

quarternary amines, which are already positively charged. Overton concluded that it is the neutral weak base, rather than the cationic acidic form, that predominantly enters the cell. Overton subsequently studied the uptake of acids into frog muscle, using osmotic swelling to gauge solute influx. He found that neutral weak acids (e.g. acetic acid) were far more effective than more acidic solutions of strong acids, again leading him to conclude that the neutral species more easily crossed into cells, and supporting his insightful hypothesis that the cell membrane consists predominantly of lipids.

Confirmation with NH_3 . By studying cells containing native or exogenously applied pH-sensitive dyes, other investigators confirmed Overton's fundamental observations on a wide range of cell types. For example, several investigators showed that an exposure to $\text{NH}_3/\text{NH}_4^+$ causes internal pH to rise (Warburg, 1910; Harvey, 1911; Jacobs, 1922). In more modern times, Roger Thomas in 1974 used a microelectrode to show that an exposure to $\text{NH}_3/\text{NH}_4^+$ causes the intracellular pH (pH_i) of a snail neuron to rise, and that the removal of extracellular $\text{NH}_3/\text{NH}_4^+$ has the opposite effect (Thomas, 1974). In 1976, Boron and De Weer extended these observations in microelectrode experiments on squid axons (Boron & De Weer, 1976b), as illustrated by the twin-pulse experiment shown in Fig. 1A. In the brief, first exposure, pH_i rises monotonically as the entry of the weak base NH_3 leads to the consumption of intracellular H^+ and the formation of NH_4^+ , as illustrated in Fig. 1B. After the removal of $\text{NH}_3/\text{NH}_4^+$, the reactions in Fig. 1B reverse and pH_i falls but, curiously, to a value that modestly undershoots the initial pH_i .

In the longer, second $\text{NH}_3/\text{NH}_4^+$ exposure shown in Fig. 1A, one might have thought that pH_i should gradually approach an asymptote as $[\text{NH}_3]_i$ gradually approaches extracellular $[\text{NH}_3]$ or $[\text{NH}_3]_o$. Instead, pH_i rises to a peak and then begins a slower decline. This plateau-phase acidification is due to the entry of the weak acid NH_4^+ . As shown in Fig. 1C, a small fraction of the entering NH_4^+ dissociates in the cytosol to form H^+ and NH_3 . As $[\text{NH}_3]_i$ rises above $[\text{NH}_3]_o$, NH_3 exits the cell and combines with extracellular H^+ to form NH_4^+ , which completes the cycle by entering the cell. Thus, during the plateau phase, NH_3 effectively shuttles H^+ into the cell. Even during the brief $\text{NH}_3/\text{NH}_4^+$ exposure in Fig. 1A, the influx of NH_4^+ , overwhelmed by the entry of NH_3 , must have slowed the rate of pH_i increase, reduced the magnitude of the overall NH_3 -induced pH_i increase and led to a modest, excess build up of intracellular NH_4^+ . Upon removal of the extracellular $\text{NH}_3/\text{NH}_4^+$, this excess intracellular NH_4^+ dissociates into NH_3 , which leaves the cell, plus H^+ , which causes the modest pH_i undershoot. In the longer $\text{NH}_3/\text{NH}_4^+$ exposure, the much larger build

up of intracellular NH_4^+ leads to a correspondingly greater pH_i undershoot.

The above work introduced the so-called ammonium-prepulse technique, which has become a widely used method for acid loading cells.

Depending on the cell type, a plateau-phase acidification like that in Fig. 1A can reflect the action of any of several mechanisms that acidify the cell. In barnacle muscle fibres, NH_4^+ entry through channels, presumably K^+ channels, plays a major role (Boron, 1977; Kikeri *et al.* 1989). As discussed below, the $\text{Na}^+ - \text{K}^+$ pump can take up NH_4^+ , especially when $[\text{K}^+]_o$ is low (Aickin & Thomas, 1977), and the $\text{Na}^+ - \text{K}^+ - 2\text{Cl}^-$ cotransporter can also mediate a robust uptake of NH_4^+ (Kinne *et al.* 1986; Kikeri *et al.* 1989). In fact, because of similarities in the physicochemical properties of NH_4^+ and K^+ in aqueous solution, any K^+ -transport pathway could be viewed as a potential means of NH_4^+ transport. Finally, in the presence of $\text{CO}_2/\text{HCO}_3^-$, the $\text{Cl}^- - \text{HCO}_3^-$ exchanger (a pH_i -regulatory mechanism that is called into play when pH_i is too high) can make a contribution to the plateau-phase acidification (Vaughan-Jones, 1982). Regardless of the mechanism of the plateau-phase acidification, all work summarized above is consistent with Overton's view that the neutral weak base is the dominant species that moves through the membrane.

Confirmation with CO_2 . After Overton, Jacobs, using the native pH-sensitive dye in flower petals, confirmed Overton's results by demonstrating that the cells exposed to $\text{CO}_2/\text{HCO}_3^-$ underwent a fall in internal pH (Jacobs, 1920). Caldwell, working on squid axons, was the first to observe a CO_2 -induced fall of pH_i using a pH-sensitive microelectrode (Caldwell, 1958), and Thomas, working on snail neurons with his newly designed glass microelectrode that was truly 'micro', was the first to show that the acidifying effect of CO_2 is reversible (Thomas, 1974).

In their experiments on squid axons, Boron & De Weer (1976b) extended the earlier work by lengthening the time of the $\text{CO}_2/\text{HCO}_3^-$ exposure. As shown in Fig. 2A, pH_i at first falls rapidly as the entry of CO_2 leads to the formation of intracellular carbonic acid, which in turn dissociates to form intracellular H^+ and HCO_3^- , as illustrated in Fig. 2B. Although one might expect that pH_i would gradually approach an asymptote as $[\text{CO}_2]_i$ gradually approaches $[\text{CO}_2]_o$, pH_i begins a slow increase that can only be explained by 'acid extrusion', the active removal of an acid (e.g. H^+) or the active uptake of a base (e.g. HCO_3^-), as shown in Fig. 2C. Either way, acid extrusion would lead to the accumulation of excess HCO_3^- inside the cell. With the subsequent removal of extracellular $\text{CO}_2/\text{HCO}_3^-$, the excess intracellular HCO_3^- combines with H^+ and eventually exits the cell as CO_2 , producing the overshoot in Fig. 2A.

The experiment in Fig. 2A was the first example of the dynamic regulation of pH_i . It had been surmised since the work of Fenn that, in the steady state, cells faced with the passive influx of H^+ must extrude acid in order to maintain the observed pH_i (Fenn & Cobb, 1934; Fenn & Maurer, 1935). In 1975, Roos took the next important step in the field of pH_i regulation, when he exposed rat diaphragm muscle to either D-lactic acid ($\text{HLac} \rightleftharpoons \text{H}^+ + \text{Lac}^-$) or the weak acid DMO ($\text{HDMO} \rightleftharpoons \text{H}^+ + \text{DMO}^-$). He confirmed that, after a few hours, the cells had accumulated large amounts of

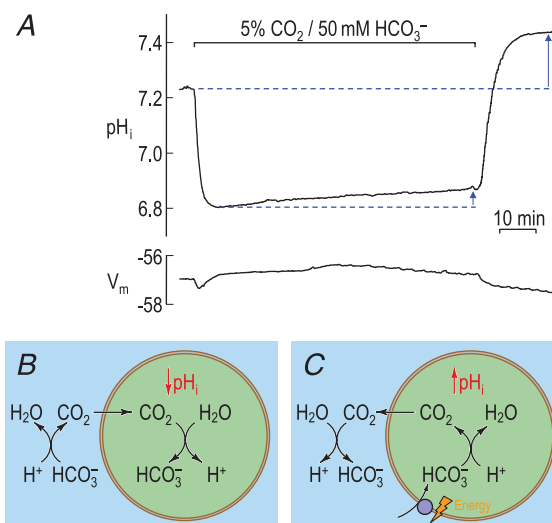


Figure 2. Effect of extracellular $\text{CO}_2/\text{HCO}_3^-$ on intracellular pH of a squid giant axon, showing data (A), model of acidifying phase (B) and model of alkalization during plateau phase (C) Throughout the experiment in A, ASW with an extracellular pH of 7.70 flowed past a cannulated axon, which was suspended in a chamber of small volume. Intracellular pH and membrane potential were monitored with glass microelectrodes. During the indicated period, the ASW was switched to one equilibrated with 5% CO_2 and in which 50 mM NaHCO_3 replaced 50 mM NaCl . Data are from Boron & De Weer (1976b). B shows that the influx of CO_2 leads to the production of intracellular H^+ and thus a fall in pH_i . This process accounts for the falling phase of pH_i during the $\text{CO}_2/\text{HCO}_3^-$ exposure in A. The influx of CO_2 in B leads to the indicated reaction near the extracellular surface of the membrane. In the bulk (i.e. flowing) ASW, the $\text{CO}_2/\text{HCO}_3^-$ buffer was in equilibrium ($\text{CO}_2 + \text{H}_2\text{O} \rightleftharpoons \text{H}^+ + \text{HCO}_3^-$). C shows the system after CO_2 has equilibrated across the cell membrane; this equilibration corresponds to the pH_i nadir during the $\text{CO}_2/\text{HCO}_3^-$ pulse. After this equilibration, pH_i is dominated by 'acid extrusion', shown here as the active uptake of HCO_3^- . This active uptake of HCO_3^- is mediated by a transporter called a Na^+ -driven $\text{Cl}^- - \text{HCO}_3^-$ exchanger (which may mediate uptake of CO_3^{2-} or NaCO_3^- ion pair). This HCO_3^- uptake had been occurring since the beginning of the $\text{CO}_2/\text{HCO}_3^-$ exposure, but its effect on pH_i had been overwhelmed by the influx of CO_2 . Now, during the plateau phase, HCO_3^- uptake leads to a consumption of H^+ in the cytosol and thus the production of CO_2 , leading to a net efflux of CO_2 . This process accounts for the plateau-phase alkalization (i.e. rising phase of pH_i) during the $\text{CO}_2/\text{HCO}_3^-$ exposure in A. Because the cell accumulated HCO_3^- during the $\text{CO}_2/\text{HCO}_3^-$ exposure, the removal of extracellular $\text{CO}_2/\text{HCO}_3^-$ leads to a pH_i overshoot.

D-lactate or DMO⁻, which implied, if the permeant species were H₂Lac or HDMO, that the cytosol had undergone a massive acid load. Nevertheless, he found that the simultaneously computed p*H*_i was near the value of muscle fibres not so acid loaded. He correctly concluded that the cells, between the time of the acid load and the measurement of p*H*_i, must have extruded the H⁺ load (Roos, 1975). The experiment in Fig. 2*A* directly demonstrated the sorts of processes that Roos had envisioned, and also revealed the time courses; a relatively rapid intracellular acid load, followed by a slower p*H*_i recovery due to an active process.

Later work in both the squid axon and the snail neuron demonstrated that the acid-extrusion mechanism in squid axons and snail neurons is due to a Na⁺-driven Cl⁻-HCO₃⁻ exchanger (Boron & De Weer, 1976*a*; Russell & Boron, 1976; Thomas, 1976, 1977; Boron & Russell, 1983). In many other cells studied in the absence of CO₂/HCO₃⁻, the p*H*_i recovery from an acid load is mediated by a Na⁺-H⁺ exchanger, as first demonstrated by Aickin & Thomas (1977) for mouse skeletal muscle. The Na⁺-H⁺ exchanger had previously been demonstrated in membrane vesicles from small intestine and kidney by Murer *et al.* (1976), who approached the issue from the perspective of transepithelial transport. For a more in-depth treatment of the role of these transporters in p*H*_i regulation, the reader might consult reviews specifically on that topic (Roos & Boron, 1981; Boron, 2004; Bevensee & Boron, 2008; Vaughan-Jones *et al.* 2009; Casey *et al.* 2010).

Cautionary notes on p*H*. In his experiments, Overton measured the ability of an entering substance either to precipitate tannins or to cause osmotic swelling, both of which are reasonably direct measures of influx. The same cannot be said of the far more common, modern assays that exploit measurements of p*H*_i (e.g. Figs 1 and 2). These assays do not assess permeability *per se* but whether it is the neutral *versus* charged species of a buffer pair that has the dominant impact on p*H*_i. However, conclusions in the literature are almost never stated in this limited manner. For example, the NH₃-induced alkalinization in Fig. 1 does not prove that the cell membrane is impermeable to NH₄⁺; in fact, the membrane is permeable to NH₄⁺, which is the basis for the plateau-phase acidification in Fig. 1. In fact, such experiments do not even prove that the NH₃ flux is greater than the NH₄⁺ flux. As discussed in greater length elsewhere (Musa-Aziz *et al.* 2009*c*), one can conclude from Fig. 1 only that the ratio of the NH₃ influx (*J*_{NH₃}) to the NH₄⁺ influx (*J*_{NH₄⁺}) exceeds 10^(p*H*_i - p*K*), a conclusion that flows from the analysis in the appendix of the paper by Boron & De Weer (1976*b*). For example, if p*H*_i is 7.3 and the p*K* of the NH₃-NH₄⁺ equilibrium is 9.3, exposing a

cell to an NH₃/NH₄⁺ solution will cause p*H*_i to rise when:

$$\frac{J_{\text{NH}_3}}{J_{\text{NH}_4^+}} > 10^{\text{pH}_i - \text{pK}} = 10^{7.3 - 9.3} = \frac{1}{100} \quad (1)$$

In other words, even if the NH₃ influx were only 1/99th of the NH₄⁺ influx, p*H*_i would still rise, albeit slowly. Note that the limiting ratio of fluxes (1/100 in this case) does not translate directly to the limiting ratio of permeabilities. For the extracellular pH (p*H*_o) values prevailing in most experiments on animal cells, [NH₃]_o << [NH₄⁺]_o. For example, in the experiment of Fig. 1, p*H*_o was 8.0 and thus the ratio [NH₃]_o/[NH₄⁺]_o was 1/20 or fivefold greater than the limiting ratio of fluxes. If we imagine that membrane potential (*V*_m) were zero (so that we could ignore the effects of charge on the diffusion of NH₄⁺), p*H*_i would rise as long as the permeability ratio *P*_{NH₄⁺}/*P*_{NH₃} were <5. Thus, if *P*_{NH₄⁺}/*P*_{NH₃} were, say, 4, then the 20-fold advantage in NH₄⁺ concentration and fourfold advantage in NH₄⁺ permeability would produce only an 80-fold advantage for the influx of NH₄⁺ over NH₃, which is still below the value of 100-fold necessary to stem the alkalinizing effect of NH₃ on p*H*_i.

We could use similar logic in analysing the CO₂-induced acidification in Fig. 2. Here, one can conclude only that the ratio of CO₂ influx (*J*_{CO₂}) to HCO₃⁻ influx (*J*_{HCO₃⁻}) exceeds 10^(p*H*_i - p*K*). Thus, if p*H*_i is 7.3 and the p*K* of the CO₂-HCO₃⁻ equilibrium is 6.1, exposing a cell to a CO₂/HCO₃⁻ solution will cause p*H*_i to fall as long as:

$$\frac{J_{\text{CO}_2}}{J_{\text{HCO}_3^-}} > 10^{\text{pH}_i - \text{pK}} = 10^{6.1 - 7.3} \approx \frac{1}{16} \quad (2)$$

Stated differently, even if the CO₂ influx were only 1/15th of the HCO₃⁻ influx, p*H*_i would still fall.

I should emphasize that I am not attempting here to challenge the dogma that membrane lipids are more permeable to electrically neutral species (e.g. NH₃) than to their charged counterparts (e.g. NH₄⁺); the dogma is true. However, I do point out that the prevalent p*H*_i data generally do not make as strong a case for Overton's conclusions as do Overton's original data.

Overton's rule. Although Overton's work provided important insights into the predominantly lipid nature of the cell membrane (see above), today Overton is remembered for 'Overton's rule'. This principle, founded on the work of Overton and later investigators, states that membrane permeability to a substance X (*P*_{X,m}) is proportional to the oil-water partition coefficient (*K*_f) of X or, more precisely, the lipid-water partition coefficient of X (*K*_X) for the lipid of the particular membrane under consideration. Thus, if *s*_{X,aq} is the solubility of X in an aqueous solution and *s*_{X,m} is the solubility in the membrane lipid, then *K*_X = *s*_{X,m}/*s*_{X,aq}. We might regard

Overton's rule as the solubility hypothesis, as follows:

$$P_{X,m} \propto K_X \quad (3)$$

Note that $P_{X,m}$ is analogous to electrical conductance (reciprocal of resistance, R), and is only one determinant of the flux of X across the membrane (J_X). If the concentration of X in the aqueous layer in contact with the extracellular or outer surface (oS) of the membrane is $[X]_{oS, aq}$ and the concentration in the aqueous layer in contact with the intracellular or inner surface (iS) of the membrane is $[X]_{iS, aq}$, then a simplified version of Fick's law yields the following:

$$J_X = P_{X,m} ([X]_{oS, aq} - [X]_{iS, aq}) \quad (4)$$

In the next few paragraphs, we will focus on $P_{X,m}$. However, almost never do physiologists measure $P_{X,m}$ directly because they rarely have information about $[X]_{oS, aq}$ or $[X]_{iS, aq}$. Instead, physiologists generally measure the macroscopic permeability (P_X) that governs the diffusion of X from the bulk (i.e. stirred) extracellular fluid that has a known concentration of X ($[X]_{o, bulk}$), through the unstirred layer near the extracellular surface of the cell, through the membrane itself, and through an intracellular unstirred layer to some point (p) inside the cell where $[X]$ is $[X]_{i, p}$, as follows:

$$J_X = P_X ([X]_{o, bulk} - [X]_{i, p}) \dots \text{or simply} \dots \\ J_X = P_X ([X]_o - [X]_i) \quad (5)$$

Note that eqn (5) is highly oversimplified inasmuch as it ignores the following unstirred layers that envelope the cell membrane: (1) the extracellular unstirred layer (eUL) between the bulk extracellular fluid and the outer surface of the membrane; and (2) the intracellular unstirred layer (iUL) between the inner surface of the membrane and some point deeper inside the cytosol where we make our measurements.

Viewed differently, the overall 'resistance' that opposes the diffusion of X from the bulk extracellular fluid to a point in the intracellular fluid ($R_X = 1/P_X$) is the sum of the 'resistance' through the following: (1) the extracellular unstirred layer ($R_{X, eUL} = 1/P_{X, eUL}$); (2) the membrane ($R_{X, m} = 1/P_{X, m}$); and (3) the intracellular unstirred layer ($R_{X, iUL} = 1/P_{X, iUL}$). As is clear from the analysis of Pohl and colleagues (Missner *et al.* 2008*a, b*; Missner & Pohl, 2009), the combination of large unstirred layers (i.e. a relatively large sum $R_{X, eUL} + R_{X, iUL}$) and a relatively high $P_{X, m}$ (i.e. a relatively small $R_{X, m}$) renders P_X virtually insensitive to modest changes in $P_{X, m}$. In other words, the permeability of the membrane *per se* only matters if $P_{X, m}$ is relatively small compared with the aggregate permeability of the unstirred layers. We might term this the series-resistance problem, which we will consider again below (section 'A view from artificial bilayers').

Consideration of the diffusion constant. Over the decades, Overton's hypothesis evolved into Overton's rule. However, even as the rule became firmly cemented in our physiology textbooks, it became clear to the practitioners of membrane biology that the solubility hypothesis is overly simplistic. For example, many small molecules are more permeable than expected, with the increase being inversely related to molecular volume (Walter & Gutknecht, 1986). Biologists recognized that the permeability of substance X through the membrane depends not only on solubility but also the diffusion constant (D_X). We might term this is the solubility-diffusion hypothesis (see Finkelstein, 1986), as follows:

$$P_{X,m} \propto K_X \times D_X \quad (6)$$

The spirit of eqn (6) is clearly reflected in a physiology textbook with which I am intimately familiar (see Boron & Boulpaep, 2009), and others before it. In other words, after dissolving in the membrane lipid, X must diffuse across the membrane. For different solutes, K_X and D_X appear to weigh differently. In the case of CO_2 transiting through artificial membranes, $P_{\text{CO}_2, m}$ appears to be more sensitive to changes in D_X than K_X . For example, CO_2 solubility varies only about twofold among a wide range of lipids, whereas CO_2 permeability has a range of over 1000 in artificial lipids (Blank & Roughton, 1960; Gutknecht *et al.* 1977; Simon & Gutknecht, 1980). Thus, D_{CO_2} must be far more important a determinant of membrane permeability than K_{CO_2} , and some lipids must have far lower D_{CO_2} values than others.

Work exploiting electron paramagnetic resonance and O_2 -sensitive spin labels concludes that adding 50% cholesterol to a dimyristoyl phosphatidylcholine (DMPC) bilayer, by reducing the local product of $[\text{O}_2]$ and D_{O_2} within the membrane, can reduce membrane O_2 permeability by 75–80% of the value in a pure DMPC membrane (Subczynski & Swartz, 2005).

As an historical aside, chemists studying the diffusion of gases through polymers were, alas, well out in front of the physiologists. According to one review (Stannett, 1978), John Kearsley Mitchell had formulated what we now call 'Overton's rule' in 1831, well over a half century before Overton's experiments. The physical chemist Thomas Graham, who gave us Graham's law, discovered dialysis and is considered the founder of colloid chemistry, published his first paper on gas transport across membranes in 1829. He enunciated the solubility-diffusion theory in 1866, about a century before biologists.

Consideration of integral membrane proteins. Integral membrane proteins could reduce permeability by at least three general mechanisms.

First, it is important to recognize a trivial principle, that substances cannot dissolve in membrane lipid that is not there, having been displaced by integral membrane proteins that typically make up 25% of the membrane surface area. This figure is 50% or more in the erythrocyte (see Forster *et al.* 1998) and is presumably even higher in the membrane of the astrocytic end-foot that faces CNS vessels (these membranes consist of ~35% aquaporin (AQP) 4 in semi-crystalline arrays; see Amiry-Moghaddam *et al.* 2004). A space-filling model of the synaptic vesicle (which identified only about half of the proteins) shows that the structure is ‘dominated’ by membrane proteins (see Fig. 4 of Takamori *et al.* 2006). Although a particular integral membrane protein may transport a restricted set of substances, we can generally regard any such protein as being an absolute barrier to most substances. An electron paramagnetic resonance study of O₂ permeability suggests that, merely by displacing lipids, integral membrane proteins can reduce overall membrane permeability to half to a third of the value in an artificial lipid bilayer (Subczynski & Swartz, 2005).

A second mechanism by which integral membrane proteins can reduce permeability is by organizing the surrounding lipids (Engelman, 2005; Subczynski & Swartz, 2005; Subczynski *et al.* 2009). Electron paramagnetic resonance studies of O₂ permeability indicate that integral membrane proteins reduce O₂ permeability by creating slow oxygen transport (SLOT) domains in which O₂ permeability can be reduced to 1/16 that of bulk-lipid domains in the same membrane (Kawasaki *et al.* 2001). At least in the example of the influenza virus membrane, the ratio of SLOT/bulk lipids is ~40%/60%.

Together, mechanisms 1 and 2 reduce K_X and D_X to the effective values K'_X and D'_X . We might term our updated model, which includes the ability of integral membrane proteins to displace and organize lipids, the solubility-diffusion-protein hypothesis, expressed as follows:

$$P_{X,m} \propto K'_X \times D'_X \quad (7)$$

The third mechanism by which integral membrane proteins can reduce permeability is by contributing to the reduction of access/egress as discussed in the following section.

Consideration of access to and egress from the membrane lipid. In addition to solubility, diffusion and integral membrane proteins, I would add a third consideration, that solubilization and diffusion (as modulated by integral membrane proteins) are only possible after the substance has gained access to the membrane lipid, and can continue only if the solute can exit the membrane. We might term this the access-solubility-diffusion-protein-egress

hypothesis, as follows:

$$P_{X,m} \propto (\text{Access/egress efficiency}) \times K'_X \times D'_X \quad (8)$$

Access/egress efficiency is almost certainly not 100%. Integral membrane proteins presumably reduce access/egress by at least two mechanisms. First, as pointed out by Engelman, even integral membrane proteins with modest cross-sectional areas in the plane of the lipid bilayer can have impressive ‘ectodomains covering lipid and creating steric restrictions’ (Engelman, 2005). Second, integral membrane proteins can form complexes with soluble proteins. As in the case of the large ectodomains, if a soluble-but-bound protein literally abuts the lipid, it insulates the lipid surface from the aqueous solution. If the protein hovers some distance from the membrane, it restricts diffusion by increasing the tortuosity factor between the bulk fluid and the lipid surface.

Some soluble proteins can attach to the membrane lipid, independent of integral membrane proteins, via ionic or hydrophobic interactions. These attached proteins, and other soluble proteins that attach to them, could restrict access/egress to/from membrane lipids as outlined above for the ectodomains of integral membrane proteins and for soluble proteins adhering to these ectodomains. The plasma membrane, particularly the inner surface with its phosphatidyl serine (Subczynski & Swartz, 2005) and phosphoinositides, is the major locus of the cell’s negative membrane-surface charge and strongly attracts soluble polycationic proteins (see Leventis & Grinstein, 2010).

Even those phospholipid head groups not masked by proteins can locally organize water molecules and thereby create an energy barrier to CO₂ entry into/exit from lipid membranes (Wang *et al.* 2007). Sugar polymers attached to the outer surface of the plasma membrane could also reduce access to membrane lipid.

Overall effect on background membrane permeability.

It may be worth noting that, whereas D_X is a kinetic term that describes the rate of diffusion, the lipid-water partition coefficient is a thermodynamic term that describes, at equilibrium, the concentration ratio of substance X in membrane lipid to water. The term K_X says nothing about the speed with which X reaches its equilibrium concentration in membrane lipid. Thus, K_X does not define the concentration of X at any distance through the membrane lipid, but the maximal possible [X] at infinite time with equal [X] on opposite sides of the membrane. While X is entering a cell, for example, the [X] at any distance through the thickness of the membrane lipid (i.e. around proteins in the plane of the membrane) depends on the following: (1) [X] in the aqueous layer near the extracellular surface of the membrane; (2) access efficiency; (3) the kinetics of solubilisation; (4) the effective K_X (which determines the

upper bound of [X] in lipid) as reduced by integral membrane proteins; (5) the effective diffusion constant within the membrane lipid as reduced by integral membrane proteins; (6) the kinetics of desolubilization; (7) egress efficiency; and (8) [X] in the aqueous layer near the intracellular surface of the membrane. In other words, the solubility hypothesis (i.e. Overton's rule) merely sets an upper bound on the permeability properties of the lipid portion of the membrane, and cannot predict how far below this theoretical maximum the permeability may be in the lipid phase of a real biological membrane in various physiological conditions.

By how much might the presence of integral membrane proteins and the presence of cholesterol in bulk membrane lipids reduce 'background' membrane permeability? If proteins occupied two-thirds of the membrane surface, if 40% of the lipids were protein associated (assumed 1/16 of normal lipid permeability), and if 60% of the lipids had a 50% molar ratio of cholesterol (assumed 1/5 of normal lipid permeability), then the background permeability might fall to ~5% of the nominal value. Reduced access/egress efficiency caused by ectodomains of integral membrane proteins and by adherent soluble proteins could further reduce this figure.

Chinks in Overton's armour

Despite the cautionary notes in the previous section, in the early 1990s I did not know anyone, including me, who questioned Overton's rule, or the implicit dogma that all gases move through all membranes simply by dissolving in the lipid phase of the membrane. According to this philosophy, gas transport depends only on concentration gradients and the properties of the lipid phase of the membrane, leaving no possibility of regulation, and little possibility of selectivity beyond what might be allowed by solubility-diffusion theory. But then things began to change. . . .

Membranes with relatively low $\text{NH}_3/\text{NH}_4^+$ permeability ratios. Hamm *et al.* (1985) demonstrated that the apparent transepithelial NH_3 permeability of the isolated, perfused cortical collecting tubule is much lower than for proximal convoluted tubules ($\sim 5 \times 10^{-3}$ versus $\sim 6 \times 10^{-2}$ cm s^{-1}), which was perhaps the first argument consistent with restricted NH_3 permeation. However, sceptics might argue that the difference could reflect the much higher surface area of proximal-tubule cells.

Garvin *et al.* (1988) examined the transepithelial permeability of NH_3 versus NH_4^+ in renal thick ascending limb (TAL). This nephron segment is peculiar, and important, because its apical membrane (i.e. the one facing the lumen) has a very low permeability to H_2O . Thus, the reabsorption (i.e. movement from lumen to

blood) of NaCl by the TAL is disproportionately high compared with the reabsorption of H_2O , leaving behind in the lumen a relative surplus of H_2O (hence, the term 'diluting segment') and simultaneously creating a hypertonic interstitium. The TAL also plays a critical role in transferring NH_4^+ from the lumen to the interstitium and then short-circuiting it to the collecting ducts for excretion in the urine. Garvin and colleagues found that the apparent transepithelial NH_3 permeability of the TAL, like that of the cortical collecting tubule, is quite low ($\sim 3.1 \times 10^{-3}$ cm s^{-1}). However, more telling was the observation that this value was only about 20-fold greater than the transepithelial NH_4^+ permeability ($\sim 1.5 \times 10^{-4}$ cm s^{-1}), far lower than one would predict by Overton's rule. These data are consistent with the hypothesis that the TAL epithelium either restricts the diffusion of NH_3 and/or enhances the transport of NH_4^+ via channels/transporters.

Kikeri *et al.* (1989) extended the work of Garvin and colleagues by monitoring the pH_i of TAL cells while introducing $\text{NH}_3/\text{NH}_4^+$ to the lumen. Rather than the usual initial rise in pH_i , they observed only a sustained fall. Aickin & Thomas (1977) had observed a large and sustained acidification in the presence of extracellular $\text{NH}_3/\text{NH}_4^+$, but only after replacing extracellular K^+ with NH_4^+ (presumably forcing the Na^+-K^+ pump to carry NH_4^+ , rather than K^+ , into the cell), and even then they sometimes observed a small transient rise in pH_i (due to NH_3 entry). Thus, Kikeri and coworkers demonstrated for the first time, in more-or-less physiological conditions, that the effects of NH_4^+ influx can overwhelm those of NH_3 influx from the perspective of pH_i . By analogy with eqn (1), we can conclude the following:

$$\frac{J_{\text{NH}_3}}{J_{\text{NH}_4^+}} < 10^{\text{pH}_i - \text{pK}} \approx \frac{1}{100} \quad \text{or} \quad \frac{J_{\text{NH}_4^+}}{J_{\text{NH}_3}} > 10^{\text{pK} - \text{pH}_i} \approx 100 \quad (9)$$

These inequalities are consistent with the earlier data of Garvin *et al.* (1988). Despite the title of the Kikeri paper, one cannot really conclude from the data that the apical membrane of the TAL cells is impermeable to NH_3 , only that the flux of NH_4^+ , carried by apical $\text{Na}^+-\text{K}^+-2\text{Cl}^-$ cotransporters and K^+ channels, greatly dominates over that of NH_3 from the perspective of pH_i .

A membrane with no detectable permeability to NH_3 or NH_4^+ . In 1989, surgical resident Steven Waisbren approached me with the idea of studying pH_i regulation in gastric parietal cells. The initial suggestion was to dissociate these cells from gastric glands and study them in isolation. I remember my almost reflex-like response, 'Not in my lab!' . . . with the explanation that these are epithelial cells and it is important to respect their sidedness. This instinct proved to be critical. We decided

to hand-dissect single glands from the fundus of a rabbit stomach (Waisbren *et al.* 1994a) and to perfuse the isolated gland as one would a renal tubule (Burg *et al.* 1966). Waisbren sucked up the blind end of a rabbit gland into a pipette assembly and pierced the base of the gland with the perfusion pipette, thereby initiating perfusion in the orthograde direction. The challenge is that the gastric-gland lumen is not so much the inside of a garden hose as it is a twisting ribbon.

Waisbren's first goal was to acid load the cells using an NH_4^+ prepulse (see Fig. 1) and then examine the pH_i recovery from the acute acid load. Owing to the plumbing of the perfusion-pipette system, the user-initiated switching of luminal solutions entails a lengthy (e.g. ~ 20 s) and somewhat variable delay before the new solution (in this case, the one containing 20 mM

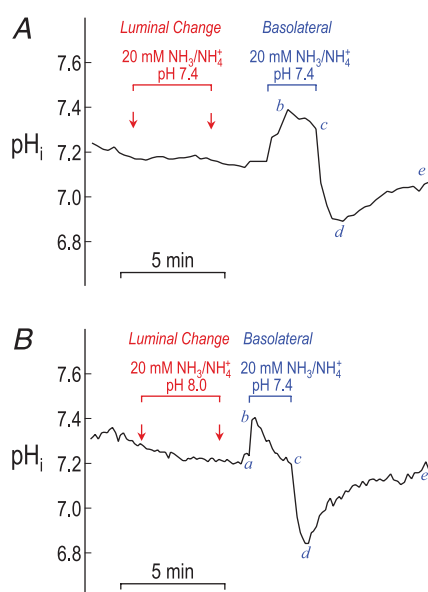


Figure 3. Effect of luminal versus basolateral $\text{NH}_3/\text{NH}_4^+$ on intracellular pH of parietal cells of isolated, perfused gastric glands, with a luminal pH of 7.4 (A) and 8.0 (B)

Throughout the experiment, the lumen of the gland was perfused, and the basolateral surface ('bath') was superfused with $\text{CO}_2/\text{HCO}_3^-$ -free physiological saline at 37°C . Intracellular pH of multiple parietal and chief cells was measured using the pH-sensitive dye BCECF in conjunction with a digital-imaging system. Data are from Waisbren *et al.* (1994b); similar data were obtained on chief cells. During the indicated periods, either the luminal or the basolateral solution was switched to one in which 20 mM NH_4Cl replaced 20 mM NaCl. In A, both luminal and basolateral $\text{NH}_3/\text{NH}_4^+$ solutions had a pH of 7.4. In B, the luminal $\text{NH}_3/\text{NH}_4^+$ solution had a pH of 8.0 (and thus fourfold higher $[\text{NH}_3]$), whereas the basolateral $\text{NH}_3/\text{NH}_4^+$ solution had a pH of 7.4. The basolateral $\text{NH}_3/\text{NH}_4^+$ exposures produced pH_i transients (abcd) similar to that in the second $\text{NH}_3/\text{NH}_4^+$ pulse in Fig. 1A, except that here the pH_i recovered from the acid load (de). However, the luminal exposures produced no significant pH_i changes. Together with other data, these observations showed that the apical membranes of parietal and chief cells have no detectable permeability to either NH_3 or NH_4^+ .

$\text{NH}_3/\text{NH}_4^+$) arrives in the lumen. Thus, it was our practice when working with proximal tubules first to switch the luminal solution, wait for pH_i to begin to rise (indicating arrival of NH_3 in the lumen), and then to switch the basolateral or 'bath' solution (which arrives with predictable rapidity). Employing this protocol with a gastric gland, Waisbren switched the luminal solution from our standard Hepes-buffered saline at pH 7.40 to an otherwise identical solution in which he replaced 20 mM NaCl with 20 mM $\text{NH}_3/\text{NH}_4^+$ and he waited . . . and waited for pH_i to rise.

Waisbren called to me several minutes after he had initiated that luminal solution switch, and announced the unexpected null result. We then watched together as he switched the basolateral solution to one containing 20 mM $\text{NH}_3/\text{NH}_4^+$, and observed the 'usual' series of pH_i changes for an ' NH_4^+ prepulse'. Figure 3A shows a parietal-cell pH_i record from such an experiment (Waisbren *et al.* 1994b). Note that, during the first part of the experiment, luminal $[\text{NH}_3]$ was ~ 0.40 mM (at pH 7.4, $[\text{NH}_3]/[\text{NH}_4^+] = 0.4/19.6 \approx 0.02$) but did not cause a change in pH_i . However, the same solution applied to the bath elicited pH_i transients typical of an NH_4^+ prepulse (segments abcde). Figure 3B shows a similar experiment, but one in which—during the exposure to 20 mM luminal $\text{NH}_3/\text{NH}_4^+$ —the luminal pH was 8.00 (rather than 7.40). Thus, luminal $[\text{NH}_3]$ was ~ 1.46 mM ($[\text{NH}_3]/[\text{NH}_4^+] = 1.46/18.54 \approx 0.08$). Nevertheless, although the $[\text{NH}_3]/[\text{NH}_4^+]$ ratio was about fourfold higher than in Fig. 3A, pH_i still did not change during the luminal exposure to $\text{NH}_3/\text{NH}_4^+$. In still other experiments (not shown), Waisbren replaced all 135 mM luminal Na^+ with 135 mM $\text{NH}_3/\text{NH}_4^+$ at pH 7.4 ($[\text{NH}_3]/[\text{NH}_4^+] \approx 0.08$ but at much higher $[\text{NH}_3]$ and $[\text{NH}_4^+]$ values than in Fig. 3A) but pH_i still did not budge. He obtained similar results from gastric chief cells.

Assuming that the above experiments were technically correct, can we explain the absence of a luminal- $\text{NH}_3/\text{NH}_4^+$ -induced pH_i change on the basis of serendipitous combinations of NH_3 and NH_4^+ influxes across the apical membrane? We need only consider the case of parallel influxes of NH_3 and NH_4^+ . Parallel effluxes are probably impossible, given the absence of both NH_3 and NH_4^+ in the basolateral solution. Fluxes of NH_3 and NH_4^+ in opposing directions would always produce a pH_i change, with pH_i falling with an NH_3 influx and rising with an NH_3 efflux (Boron & De Weer, 1976b). By analogy with eqn (1), and as discussed elsewhere (Musa-Aziz *et al.* 2009c), we can define a ratio of NH_3 and NH_4^+ fluxes that would produce no change in pH_i as follows:

$$\left(\frac{J_{\text{NH}_3}}{J_{\text{NH}_4^+}} \right)_{\text{Null}} = 10^{\text{pH}_i - \text{pK}_a} \quad (10)$$

Even if the condition prescribed in eqn (10) (that is, $(J_{\text{NH}_3}/J_{\text{NH}_4^+})_{\text{Null}} \approx 1/100$) were satisfied in Fig. 3A when luminal (L) pH was 7.4 and luminal $[\text{NH}_3]/[\text{NH}_4^+]$ was ~ 0.02 , is it reasonable to expect the same equation to be satisfied in Fig. 3B when pH_L was 8.0 and $[\text{NH}_3]_L/[\text{NH}_4^+]_L$ was ~ 0.08 ? In the latter case, $[\text{NH}_3]_L$ was about fourfold higher and $[\text{NH}_4^+]_L$ was somewhat reduced. Moreover, in the case with 135 mM $\text{NH}_3/\text{NH}_4^+$ in the lumen, we would have expected NH_4^+ transport through a transporter or a channel eventually to saturate and thus shift $(J_{\text{NH}_3}/J_{\text{NH}_4^+})$ away from $(J_{\text{NH}_3}/J_{\text{NH}_4^+})_{\text{Null}}$. Thus, it is difficult to escape the conclusion that the apical membranes of both parietal and chief cells, exposed to perhaps the most hostile environment in the body, have an undetectably low permeability to both NH_4^+ and NH_3 .

A membrane with no detectable permeability to CO_2 or HCO_3^- . In the same study as that discussed above in conjunction with Fig. 3, Waisbren examined the effects of exposing the apical and basolateral membranes to $\text{CO}_2/\text{HCO}_3^-$ (Waisbren *et al.* 1994b). The initial portion of Fig. 4A shows that a basolateral exposure to 5% $\text{CO}_2/22$ mM HCO_3^- (pH 7.40) produces a rapid CO_2 -induced fall in pH_i (segment *ab*) followed by a slower recovery (segment *bc*) that reflects the pH_i -regulatory activity of this gastric parietal cell. The removal of the basolateral $\text{CO}_2/\text{HCO}_3^-$ causes a pH_i increase (segment *cd*) due to CO_2 efflux followed by a pH_i relaxation (following segment *d*). A subsequent exposure to luminal 5% $\text{CO}_2/22$ mM HCO_3^- at the same pH of 7.40 had no effect on pH_i . Figure 4B shows an experiment in which Waisbren blocked pH_i regulation with 200 μM 4,4'-diisothiocyanatostibene-2,2'-disulfonic acid (DIDS) in order to detect small CO_2 -induced pH_i decreases more easily. His first manoeuvre, introducing 100% $\text{CO}_2/22$ mM HCO_3^- (pH ~ 6.1) into the lumen, had no effect on pH_i . Nevertheless, subsequent basolateral exposures to 1% $\text{CO}_2/\text{HCO}_3^-$ and 5% $\text{CO}_2/\text{HCO}_3^-$ produced graded CO_2 -induced decreases in pH_i but no pH_i recovery. Waisbren obtained similar results on chief cells. Comparable to the $\text{NH}_3/\text{NH}_4^+$ data, luminal CO_2 did not acidify cells even though the $\text{CO}_2/\text{HCO}_3^-$ ratio varied by a factor of ~ 20 between Fig. 4A and B. Thus, it is not clear how a fortuitous combination of CO_2 and HCO_3^- influxes could have generated a null pH_i effect in both conditions. Calculations show that, ignoring permeability to HCO_3^- , the CO_2 -permeability \times area product of the apical membrane could be no more than 1/1000 that of the basolateral membrane. We concluded that the apical membranes of gastric parietal and chief cells have no detectable permeability to either CO_2 or HCO_3^- .

Control experiments for the gastric-gland study. The above data contain several control experiments that make it unlikely that we inadvertently failed to detect a luminal CO_2 -induced pH_i decrease that was in fact there. Nevertheless, one might still argue that the permeability of the apical membranes is so high that all available NH_3 or CO_2 diffused into the gastric-gland cells in the first few micrometres of the perfused gland lumen, leaving little to enter the cells over the bulk of the gland. However, we found that all cells in the perfused gland behaved in a similar fashion. Moreover, when we perfused the lumen with an unbuffered solution containing a pH-sensitive dye, switching the luminal perfusate from 5% $\text{CO}_2/22$ mM HCO_3^- (pH 7.4) to 100% $\text{CO}_2/\text{HCO}_3^-$ (pH 6.1) caused

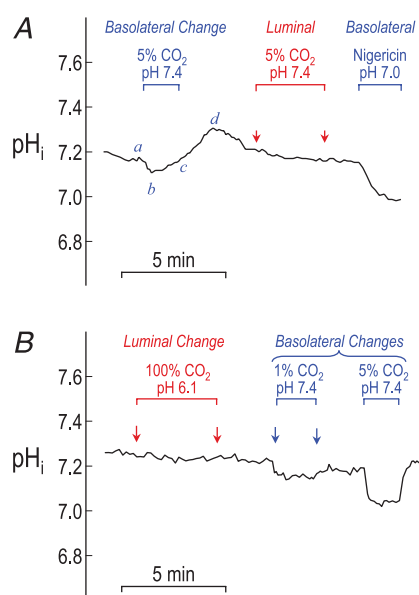


Figure 4. Effect of luminal versus basolateral $\text{CO}_2/\text{HCO}_3^-$ on intracellular pH of parietal cells of isolated, perfused gastric glands, with a luminal pH of 7.4 (A) and 6.1 (B)

Throughout the experiment, the lumen of the gland was perfused, and the basolateral surface ('bath') was superfused with physiological saline at 37°C. Intracellular pH of multiple parietal and chief cells was measured using the pH-sensitive dye BCECF in conjunction with a digital-imaging system. Data are from Waisbren *et al.* (1994b); similar data were obtained on chief cells. During the indicated periods, either the luminal or the basolateral solution was switched to one equilibrated with CO_2 . In A, both luminal and basolateral $\text{CO}_2/\text{HCO}_3^-$ solutions had a pH of 7.4 achieved with 22 mM HCO_3^- . The basolateral $\text{CO}_2/\text{HCO}_3^-$ exposures produced pH_i transients (*abcd*) similar to that in Fig. 2A. However, the luminal exposure produced no significant pH_i changes. This experiment terminated with a nigericin calibration. In B, the luminal $\text{CO}_2/\text{HCO}_3^-$ solution had a pH of 6.1 (with 100% $\text{CO}_2/22$ mM HCO_3^-) but produced no significant pH_i change. The basolateral $\text{CO}_2/\text{HCO}_3^-$ solutions had pH values of 7.4 (1% $\text{CO}_2/4.4$ mM HCO_3^- or 5% $\text{CO}_2/22$ mM HCO_3^-) and produced the expected acidifications. Basolateral 200 μM DIDS blocked the pH_i recovery from the acid loads. Together with other data, these observations showed that the apical membranes of parietal and chief cells have no detectable permeability to either CO_2 or HCO_3^- .

an abrupt fall in luminal pH along the entire gland. If CO₂ had been exiting the lumen, pH_L would have become gradually more alkaline at increasing distance from the perfusion pipette. Thus, we can conclude that, although the basolateral membranes of gastric glands have normal NH₃/NH₄⁺ and CO₂/HCO₃⁻ transport properties, the apical membranes have no detectable permeability to NH₃ or NH₄⁺, or to CO₂ or HCO₃⁻, making these the first documented gas-impermeable membranes within our limits of detection.

The apical membrane of colonic crypts. In 1995, Gastrointestinal Fellow Satish Singh published a pH_i study demonstrating that, like the cells of the rabbit gastric gland, those of the colonic crypt exhibit the normal sequence of pH_i changes when exposed to basolateral NH₃/NH₄⁺, but show no evidence of NH₃ or NH₄⁺ permeability at the apical membrane (Singh *et al.* 1995). Particularly striking was a comparison of 4 mM basolateral NH₃/NH₄⁺ at pH 7.4 ([NH₃]/[NH₄⁺] ≈ 0.02) versus 100 mM luminal NH₃/NH₄⁺ at pH 8.0 ([NH₃]/[NH₄⁺] ≈ 0.08). Even though luminal [NH₃] was ~100-fold higher than basolateral [NH₃], the basolateral exposure produced an easily discernable series of pH_i changes, where the luminal exposure was without effect. Thus, the apical membranes of colonic crypts, like those of gastric glands, also exposed to an inhospitable environment, have no detectable permeability to either NH₃ or NH₄⁺. Although not part of that study, Singh also examined in three experiments the effect of luminal CO₂/HCO₃⁻; he found no evidence of apical CO₂ permeability.

The plasma membrane of *Xenopus* oocytes. In the early 1990s, both Burckhardt & Frömter (1992) and Keicher & Meech (1994) observed that large-diameter oocytes from *Xenopus laevis*, exposed to 20 mM extracellular NH₃/NH₄⁺, exhibit a paradoxical fall in pH_i, like that first reported on other cell types by Aickin & Thomas (1977) and by Kikeri *et al.* (1989). Later, Bakouh *et al.* (2006) reported that although an exposure to 10 mM NH₃/NH₄⁺ caused oocyte pH_i to fall, an exposure to 0.5 mM NH₃/NH₄⁺ elicited no change in pH_i. As discussed below (section '*NH₃ handling by oocytes*'), work by Musa-Aziz *et al.* (2009c) using surface-pH electrodes suggests that oocytes indeed have a modest permeability to NH₃ but that the oocytes remove the incoming NH₃ from the cytosol by either metabolism or sequestration.

As demonstrated by Preston *et al.* (1992), *Xenopus* oocytes have a relatively low osmotic water permeability (P_f) except when expressing a water channel such as AQP1. From a teleological perspective, the low P_f of native oocytes is not surprising, inasmuch as amphibian blood plasma has an osmolality of ~200 mosmol kg⁻¹, whereas female *Xenopus* lay their eggs in fresh water. Thus, to the

extent that water can enter *Xenopus* oocytes by osmosis, the oocytes have a tendency to swell and ultimately burst, to the extent not compensated by some energy-requiring process. It is possible that membranes facing inhospitable environments (chemically inhospitable environments in the case of the lumen of gastric glands and colonic crypts, osmotically inhospitable in the case of *Xenopus* oocytes, or perhaps physically inhospitable environments in the case of erythrocytes) have robust membranes that render them poorly permeable to water and gases.

First evidence for gas channels: AQP1

The importance of seminars. On 17 October 1992, Peter Agre presented an elegant seminar to the Department of Cellular and Molecular Physiology at Yale, summarizing his groundbreaking work on aquaporins. Agre had first identified what proved to be the AQP1 protein in the membranes of erythrocytes and the kidney (Denker *et al.* 1988), and cloned the cDNA from human fetal liver (Preston & Agre, 1991). I was struck by the high level of AQP1 expression in erythrocyte membranes. After that seminar, Peter Agre arranged to send us the cDNA encoding AQP1 so that we could verify an earlier observation that AQP1 was not permeable to H⁺ (indeed, it was not). Later, he was quite magnanimous in sending us cDNA encoding other AQPs as well as AQP1 mutants. His generosity was critical to our early progress inasmuch as our molecular-biological skills at the time were rudimentary!

Nearly two years later, with Agre's AQP1 cDNA safely frozen away in our laboratory, I found myself presenting our recently published gastric-gland work to the Department of Physiology at the University of Pennsylvania. After the talk, someone asked me the obvious but still unanswered question, how is it that the apical membranes of gastric-gland cells are able to exclude NH₃ and CO₂? I replied that the lipids of the apical membranes may have an intrinsically low gas permeability, or contain proteins or other substances that (although not quite stated this way) reduce access/egress. As we were leaving the seminar room, Paul De Weer asked me if I considered the possibility that all membranes have an intrinsically low gas permeability, but that gastric-gland basolateral membranes have 'gas channels'; I expressed my incredulity.

Although, years later, De Weer denied any knowledge of this conversation, my mind returned to it early and often. I reasoned that if, indeed, gas channels exist, they would possess the following properties. (1) They would most probably be found in a cell whose *raison d'être* was gas transport. (2) The channel protein(s) would be present in that cell at high levels. (3) The function of the protein would either be unknown or, if known, would not

comport in an obvious way with the *raison d'être* of the cell. Before long, I realized that the cDNA for a prime candidate was languishing in our freezer. Was AQP1 not only a water channel, as so beautifully demonstrated by Agre and collaborators, but possibly also a gas channel?

Early work with CO₂ on *Xenopus* oocytes. As it happened, former postdoctoral fellow Nazih Nakhoul returned to my group from 1994 to 1995 for a sabbatical. He wished to extend his technical repertoire by performing electrophysiological experiments on *Xenopus* oocytes that were heterologously expressing mammalian proteins. As first demonstrated in the landmark paper by Preston *et al.* (1992), it is easy to express AQP1 in oocytes, and also to check the adequacy of expression by dropping them in deionized water and observing the osmotic swelling and, ultimately, a rather striking explosion. Therefore, Nakhoul decided to test the gas-channel hypothesis. With the help of Bruce Davis and Michael Romero, he injected oocytes either with cDNA encoding human AQP1 or with water as a control, and then add/removed CO₂/HCO₃⁻. In a paper published in February 1998, Nakhoul *et al.* showed that the maximal rate of CO₂-induced acidification ($[dpH_i/dt]_{\max/+CO_2}$), as well as the maximal rate of alkalization induced by the removal of CO₂ ($[dpH_i/dt]_{\max/-CO_2}$), were not different in AQP1 *versus* control oocytes (Nakhoul *et al.* 1998). We reasoned that as the CO₂ entered the cell, the reaction CO₂ + H₂O → H₂CO₃ → HCO₃⁻ + H⁺ may have been rate limiting not only for the generation of the H⁺ that the intracellular pH electrode was measuring, but also for the clearance of CO₂ from the inner surface of the cell membrane. Perhaps the latter effect, which would have reduced the inward gradient for CO₂, masked any effect of AQP1.

When he injected the oocytes with carbonic anhydrase II (CAII) protein, Nakhoul found, as expected, that rates of pH_i change were markedly increased in all conditions (e.g. 4.8-fold for CO₂ application in water-injected oocytes). Moreover, he found that during CO₂ application, when pH_i is falling rapidly, the magnitude of the CAII-dependent component of $[dpH_i/dt]_{\max/+CO_2}$ was ~45% greater in AQP1-expressing oocytes than in control oocytes injected with water rather than cRNA. During CO₂ withdrawal, when pH_i is rising rapidly, the CAII-dependent component of $[dpH_i/dt]_{\max/-CO_2}$ was ~60% greater in AQP1-expressing oocytes *versus* control oocytes. Finally, the carbonic anhydrase inhibitor ethoxzolamide (ETX) erased the effect of the CAII. The magnitude of the ETX-sensitive component of $[dpH_i/dt]_{\max/+CO_2}$ was ~65% greater for AQP1-expressing oocytes *versus* control oocytes. Thus, these experiments proved that the heterologous expression of human AQP1 causes a significant increase in the apparent CO₂ permeability of *Xenopus* oocytes. Although the most likely explanation

was that the extra CO₂ moved through AQP1, it was impossible to rule out, on the basis of the data alone, the possibility that the expression of AQP1 produced its effect by one of the following mechanisms: (1) increasing the background permeability of membrane lipids; (2) causing the upregulation of an unknown gas channel in oocytes; or (3) an effect of CAII on (1) or (2).

Later work with CO₂ on oocytes. In a paper published in December 1998, Gordon Cooper found that, in oocytes lacking exogenous CAII, the expression of AQP1 had no effect on the maximal rate of CO₂-induced acidification (Cooper & Boron, 1998), confirming the earlier work of Nakhoul *et al.* (1998). However, he found that when he removed the vitelline membrane (a manoeuvre expected to decrease the extracellular unstirred layer and thus better reveal the contribution of the cell membrane) the expression of AQP1 did indeed cause an increase in $[dpH_i/dt]_{\max/+CO_2}$. Figure 5 shows pH_i records from three oocytes, previously injected with cRNA encoding AQP1, and expressing this AQP1 to varying degrees, exposed to 1.5% CO₂/10 mM HCO₃⁻ at pH 7.50. The trace coloured purple represents the oocyte that acidified most slowly ($[dpH_i/dt]_{\max/+CO_2} = -9.6 \times 10^{-4}$ pH units s⁻¹) and, when subsequently exposed to deionized water, lysed in 180 s. Neither of these values is very different from those of water-injected control oocytes. That is, this particular oocyte, which had a low level of AQP1 expression, also had an unremarkable CO₂ permeability. The orange trace is from an oocyte that had both an intermediate acidification

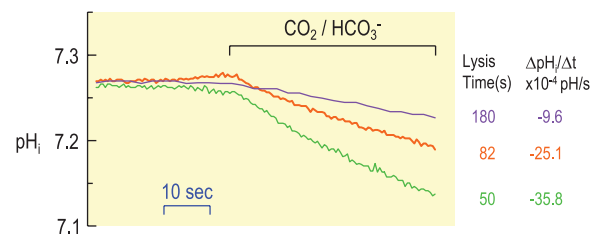


Figure 5. Effect of graded expression of human AQP1 on CO₂-induced acidification rate of *Xenopus* oocytes

Three oocytes (purple, orange and green records) injected with cRNA encoding human AQP1 were superfused with physiological saline at pH 7.5. Intracellular pH was monitored by impaling the cell with a liquid-membrane pH microelectrode and a conventional electrode for monitoring membrane potential. Data are from Cooper & Boron (1998). During the indicated periods, the extracellular solution was switched to one equilibrated with 1.5% CO₂/10 mM HCO₃⁻. The initial rate of pH_i decline is an index of the CO₂ permeability. After the electrophysiological recordings, the oocytes were dropped into deionized water and monitored for the time to lysis (shorter times correlating with greater osmotic water permeabilities). Together with other data, these observations showed that CO₂ can move through AQP1.

rate ($[\text{dpH}_i/\text{dt}]_{\text{max}/+\text{CO}_2} = -25.1 \times 10^{-4}$ pH units s^{-1}) and an intermediate lysis time (82 s). Finally, the green record is from an oocyte that acidified rapidly ($[\text{dpH}_i/\text{dt}]_{\text{max}/+\text{CO}_2} = -35.8 \times 10^{-4}$ pH units s^{-1}) and lysed quickly (50 s). A more extensive analysis of 34 devitellinized oocytes injected with cRNA encoding AQP1 demonstrated a decreasing linear relationship between the magnitude of $[\text{dpH}_i/\text{dt}]_{\text{max}/+\text{CO}_2}$ and the lysis time. In contrast, expression of the K^+ channel ROMK1 had no effect on $[\text{dpH}_i/\text{dt}]_{\text{max}/+\text{CO}_2}$ but did hyperpolarize the oocyte to the predicted equilibrium potential for potassium (E_{K}). Thus, Cooper demonstrated that CO_2 permeability correlates with the expression of AQP1 but not an unrelated K^+ channel.

Macey (1984) showed that mercurials reduce the permeability of the putative water channel in red blood cells (RBCs). In 1992, Preston and colleagues demonstrated that HgCl_2 also reduces the water permeability of AQP1 as expressed in oocytes (Preston *et al.* 1992), and in 1993 they demonstrated that Cys-189 (near the opening of the extracellular side of the water pore) is necessary for mercurial sensitivity (Preston *et al.* 1993). Therefore, Gordon Cooper examined the effect of *p*-chloromercuribenzenesulfonate (pCMBS) on the CO_2 -induced acidification. He found that pCMBS produces a larger reduction of the magnitude of $[\text{dpH}_i/\text{dt}]_{\text{max}/+\text{CO}_2}$ in AQP1-expressing oocytes than in water-injected control cells, and that this effect is abrogated by a mutation that converts Cys-189 to Ser (i.e. C189S). Thus, a mercurial derivative reduces the AQP1-dependent component of CO_2 permeability, and the predicted mutation of AQP1 prevents the inhibitory effect. These results prove that AQP1 *per se* can mediate CO_2 transport.

Work with CO_2 on erythrocytes. In December 1998, Forster *et al.* (1998) made the surprising observation that DIDS not only reduces the HCO_3^- permeability of RBCs (due to blockade of the Cl^- – HCO_3^- exchanger AE1), but the CO_2 permeability as well. The experimental approach was to use ^{18}O -labelled HCO_3^- and use mass spectrometry to monitor the degree to which carbonic anhydrase (present only inside RBCs) accelerates the loss of the ^{18}O label to H_2O . They hypothesized that DIDS could reduce CO_2 permeability by reacting either with the membrane lipid or with a major membrane protein, such as AE1 or AQP1. Citing an abstract by Cooper (a report that DIDS inhibited AQP1 expressed in oocytes; Boron & Cooper, 1998), Forster *et al.* favoured the membrane-protein option.

Work with CO_2 on reconstituted AQP1. Finally, also in December 1998, Prasad and colleagues demonstrated that human AQP1 reconstituted into *E. coli* phospholipid vesicles increased CO_2 permeability to about threefold

above background (Prasad *et al.* 1998). Mercury chloride blocked this increase in CO_2 permeability, and β -mercaptoethanol reversed the blockade. More recently, the senior author of that paper seems to have distanced himself from the conclusion that CO_2 moves through AQP1 (Missner *et al.* 2008b).

Work with nitric oxide. Herrera and colleagues (Herrera *et al.* 2006; Herrera & Garvin, 2007) demonstrated that AQP1 can also transport nitric oxide (NO). Moreover, they provided evidence that AQP1-mediated NO efflux from vascular endothelial cells, as well as AQP1-mediated NO influx into smooth-muscle cells, contributes to the full effect of endothelium-dependent vasorelaxation.

A second family of gas channels: the Rhesus (Rh) proteins

The first indication of a biological role of Rh proteins, namely, in facilitating the uptake of 'nitrogen', came from the observation that *Amt* ('ammonium transporter' in *E. coli*) and *Mep* ('methylammonium permease' in *Saccharomyces cerevisiae*) are essential for growth of microorganisms on a medium with NH_4Cl as the sole nitrogen source (Fabiny *et al.* 1991; Marini *et al.* 1994). Marini *et al.* (1997) recognized that the mammalian Rh proteins are homologous to *Mep* and *Amt* in yeast, bacteria and simple plants. They also showed that transfecting *Mep*-deficient yeast with human Rh proteins restored growth in a medium containing low ammonium (Marini *et al.* 2000). Following these critical advances, functional studies led to some discussion about whether the transported species is NH_3 , NH_4^+ , or both (see Bakouh *et al.* 2006). A key development in 2004 was the near-simultaneous determination by two groups of the X-ray crystal structure of the bacterial *AmtB*, which proved to be a homotrimer (Khademi *et al.* 2004; Zheng *et al.* 2004). The structural data strongly suggested that it is NH_3 , not NH_4^+ , that passes through the pore in each of the three *AmtB* monomers. Crystal structures are now also available for the *AmtB*–*GlnK* complex (Conroy *et al.* 2007), the fungal *Amt-1* (Andrade *et al.* 2005), the bacterial Rh50 (Lupo *et al.* 2007) and the human RhCG (Gruswitz *et al.* 2010).

Mammal Rh proteins include three erythroid proteins (RhAG, RhCE and RhD) and two non-erythroid proteins (RhBG and RhCG). Like the invertebrate Rh homologues, human RhCG is a homotrimer (Gruswitz *et al.* 2010). Moreover, an analysis of the crystal structure of RhCG, as well as of the homology of the proteins, has led to the prediction that erythroid Rh complexes are likely to be based on a template of an RhAG homotrimer, with contributions from RhCE and RhD (Gruswitz *et al.* 2010), thereby generating the experimentally determined

macroscopic ratio of about 2 RhAG: 1 RhCE: 1 RhD (Eyers *et al.* 1994).

The non-erythroid Rh proteins, RhCG and RhBG, are found in a variety of mammalian tissues, including liver, lung, stomach, gastrointestinal tract and kidney (Liu *et al.* 2001; Eladari *et al.* 2002; Quentin *et al.* 2003; Weiner & Verlander, 2003; Nakhoul & Hamm, 2004; Handlogten *et al.* 2005; Weiner, 2006; Han *et al.* 2009). In the kidney, both RhBG and RhCG are present (Liu *et al.* 2000, 2001; Marini *et al.* 2000; Eladari *et al.* 2002; Verlander *et al.* 2003; Bakouh *et al.* 2006; Ripoche *et al.* 2006; Weiner & Verlander, 2010) in both the α -intercalated cells and the principal cells of the collecting duct (CD). Here, NH_3 secretion into the lumen (in parallel with the extrusion of H^+ into the tubule lumen to lead to the formation of NH_4^+) plays an important role in urinary ' H^+ ' excretion and thus in the control of systemic pH. While RhBG is confined to the basolateral membranes (Eladari *et al.* 2002; Quentin *et al.* 2003; Verlander *et al.* 2003), RhCG is present in both the basolateral and apical membranes (Han *et al.* 2006; Seshadri *et al.* 2006; Kim *et al.* 2009). Supporting the hypothesis that RhCG is important for NH_3 secretion by the CD are the following observations: (1) RhCG-knockout mice cannot normally acidify the urine (Biver *et al.* 2008); and (2) a CD-specific RhCG knockout exhibits depressed basal NH_4^+ excretion as well as an impaired increment in NH_4^+ excretion in response to an acid load (Lee *et al.* 2009). A specific knockout of RhCG in only the intercalated cells of the CD produces a less severe deficit in NH_4^+ excretion (Lee *et al.* 2010).

The erythroid Rh complex is clinically important for blood transfusions as well as for the incompatibility that can arise between RhD-negative mothers and their RhD-positive fetuses (see Colin *et al.* 1991). The first identified function of the erythroid Rh complex was as a conduit for NH_3 (Ripoche *et al.* 2004, 2006; Bakouh *et al.* 2006; Musa-Aziz *et al.* 2009a). In addition, evidence has accumulated that the Rh complex, or simply RhAG, serves as a pathway for CO_2 (Ripoche *et al.* 2006; Endeward *et al.* 2008; Musa-Aziz *et al.* 2009a). It will be interesting to see whether the Rh complex conducts other gases, such as O_2 and NO .

Use of surface-pH measurements to study gas transport

Background. As part of another project, Raif Musa-Aziz was monitoring the surface pH (pH_s) of oocytes with a polished liquid-membrane mini-electrode (tip diameter $\sim 20 \mu\text{m}$) that she pushed up against the oocyte, dimpling the membrane slightly. She found that applying $\text{CO}_2/\text{HCO}_3^-$ in the extracellular fluid causes a predictable pH_s transient that is similar to the pH_o waveform reported long before by De Hemptinne & Huguenin (1984) in their studies on skeletal muscle. As shown in the main

portion of Fig. 6, the influx of CO_2 creates, near the outer surface of the cell membrane, a decline of $[\text{CO}_2]$ that both provides a gradient for CO_2 diffusion from the bulk extracellular fluid and, at the cell surface, drives the net reaction $\text{HCO}_3^- + \text{H}^+ \rightarrow \text{H}_2\text{CO}_3 \rightarrow \text{CO}_2 + \text{H}_2\text{O}$. The orange record in Fig. 6, for a water-injected oocyte, shows that introducing $\text{CO}_2/\text{HCO}_3^-$ causes pH_s to rise abruptly to a peak that presumably coincides with the maximal rate of CO_2 entry (Musa-Aziz *et al.* 2009a). We define the maximal magnitude of this peak as ΔpH_s . The slow pH_s decay occurs as CO_2 equilibrates across the membrane (in Fig. 2 we saw the pH_i consequences of such a slow CO_2 equilibration). The green trace in Fig. 6 shows similar results for an oocyte expressing AQP1. Since the ΔpH_s spike reflects the maximal CO_2 influx, these experiments confirm that AQP1 serves as a conduit for CO_2 .

Exposing a cell to $\text{NH}_3/\text{NH}_4^+$ causes an opposite series of pH_s changes, as first observed by Chesler in his pH_o measurements of lamprey neurons (Chesler, 1986). As illustrated in the main portion of Fig. 7, the influx of NH_3 triggers a decline of $[\text{NH}_3]_s$ that both drives NH_3 diffusion from the bulk extracellular fluid and, at the cell surface, drives the net reaction $\text{NH}_3 + \text{H}^+ \rightarrow \text{NH}_4^+$. The orange record in Fig. 7, for a water-injected oocyte, shows that introducing $\text{NH}_3/\text{NH}_4^+$ causes pH_s to fall abruptly to a nadir that presumably coincides with the maximal rate of NH_3 entry (Musa-Aziz *et al.* 2009a). The green trace in Fig. 7 shows similar results for an oocyte expressing AQP1, and confirms that AQP1 also provides a pathway for NH_3 .

These experiments show that it is rather easy to extract from pH_s transients a semi-quantitative index of maximal CO_2 or NH_3 flux, which translates to a semi-quantitative index of macroscopic permeability. In principle, this pH_s approach could work with any neutral weak acid or base. Indeed, when Musa-Aziz and colleagues (Musa-Aziz *et al.* 2009a) exposed oocytes to butyrate/butyric acid, they

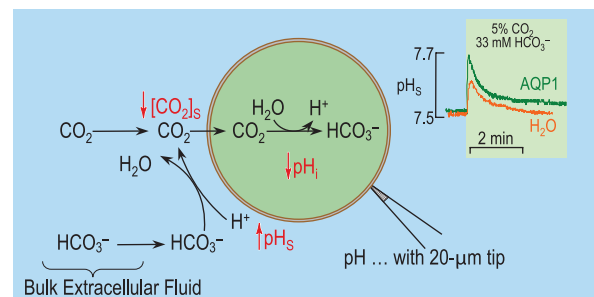


Figure 6. Model of surface pH (pH_s) changes caused by the influx of CO_2

The influx of CO_2 not only causes a fall of pH_i but also a transient rise of pH_s . The two inset pH_s records at the top right come from oocytes injected either with water or with cRNA encoding human AQP1, measured with liquid-membrane pH-sensitive microelectrodes that initially just touched the membrane surface and then were advanced an additional $\sim 40 \mu\text{m}$. Data are from Musa-Aziz *et al.* (2009a).

observed pH_S transients like those triggered by CO_2 in Fig. 6, except that AQP1 did not enhance permeability to butyric acid. However, by way of caution, I point out that it will not be trivial to extract the membrane permeability to CO_2 or butyric acid or NH_3 from pH_S transients. Colleagues at my home institution (Daniela Calvetti and Erkki Somersalo from the Department of Mathematics, as well as Rossana Occhipinti, who joined our group after completing her PhD with the Calvetti-Somersalo group) have modelled the system as a spherical cell in which reaction and diffusion processes occur simultaneously. The model seems to be reasonable from the perspective of pH_i measurements. However, it is clear that the pH_S electrode creates a special environment that accentuates pH_S transients and that more modelling will be required for a quantitative understanding of the physiology within this special environment.

Handling of NH_3 by oocytes. I have already noted that the plasma membrane of *Xenopus* oocytes is unusual (see section ‘The plasma membrane of *Xenopus* oocytes’), with oocytes responding to the application of high NH_3/NH_4^+ levels (e.g. 10–20 mM) with a paradoxical fall in pH_i , but to low NH_3/NH_4^+ levels with little change in pH_i . Musa-Aziz and colleagues re-examined this issue using, in addition to pH_i , both pH_S and NMR methods, and the new data led to the following conclusions, which are quite surprising (Musa-Aziz *et al.* 2009c). (1) Regardless of whether $[NH_3/NH_4^+]_o$ is high or low, and regardless of the presence *versus* the absence of the bacterial Rh homologue AmtB, the influx of NH_3 (rather than the influx of NH_4^+) dominates pH_S and would dominate pH_i if other factors did not come into play. (2) For these and other reasons discussed, the paradoxical fall in pH_i observed at high $[NH_3/NH_4^+]_o$ cannot be due to the influx of NH_4^+ . The pH_i decrease could result from the triggered production of intracellular H^+ . (3) AmtB enhances the influx of NH_3 over that of NH_4^+ . (4) Once it has entered the

oocyte, nearly all NH_3 appears to be sequestered as NH_4^+ , presumably in acidic compartments. (5) The removal of extracellular NH_3/NH_4^+ merely terminates, for the most part, the influx of NH_3 ; it does not, over the period of our observation, produce a large, symmetrical efflux of NH_3 . (6) A hypothetical, extracellular, low-affinity sensor for NH_3 or NH_4^+ (perhaps an adaptation that allows oocytes to survive in pond water that contains decaying organic matter) could trigger the aforementioned production of intracellular H^+ .

Gas selectivity. Armed with the pH_S approach summarized in Figs 6 and 7, Musa-Aziz and colleagues embarked on a series of experiments in which they injected oocytes with either water or cRNA encoding AQP1 (expressed at high levels in RBCs), AQP4 (highly expressed in the blood–brain barrier), AQP5 (highly expressed in alveolar type I pneumocytes), AmtB, RhAG (RBCs) or other membrane proteins. Later, they sequentially measured in each oocyte the ΔpH_S evoked by CO_2/HCO_3^- , the ΔpH_S evoked by NH_3/NH_4^+ and the osmotic water permeability. By comparing the data from oocytes expressing channels with data from day-matched water-injected control cells, they were able to obtain the following channel-dependent values (designated by*) for each oocyte: $(\Delta pH_S^*)_{CO_2}$, $(\Delta pH_S^*)_{NH_3}$ and P_f^* .

The eight panels in Fig. 8 show representative examples of CO_2 - and NH_3 -evoked pH_S transients for oocytes expressing various membrane proteins. In each case, we first exposed the oocyte to 5% $CO_2/33$ mM HCO_3^- at a fixed pH_o of 7.50 (left side of panel), then removed the CO_2/HCO_3^- (not shown), and then exposed the same oocyte to 0.5 mM NH_3/NH_4^+ at pH_o 7.50 (right side of panel). In each of the first three panels (Fig. 8A–C), we show three records (obtained on the same day from a single batch of oocytes), one from a water-injected control oocyte (the same one in each panel), one from an oocyte expressing AQP1 (again, the same oocyte in each panel) and one from an oocyte expressing the Na^+ –glucose cotransporter SGLT1 (Fig. 8A) or the Na^+ – K^+ – $2Cl^-$ cotransporter NKCC2 (Fig. 8B) or the H^+ –oligopeptide cotransporter PepT1 (Fig. 8C). For each of the three cotransporter oocytes, the pH_S record is indistinguishable from that of the water-injected control oocyte, and exhibits a ΔpH_S that is substantially less than the AQP1 oocyte. Mean data from the larger study confirm this conclusion. Thus, not every membrane protein is a gas channel.

The next group of five panels (Fig. 8D–H) shows the results of experiments on five putative gas channels, each compared with a day-matched water-injected control oocyte. Mean data from the larger study confirm the impression conveyed by these five panels. In response to the application of CO_2/HCO_3^- , all five wild-type channels produce ΔpH_S values that are significantly larger

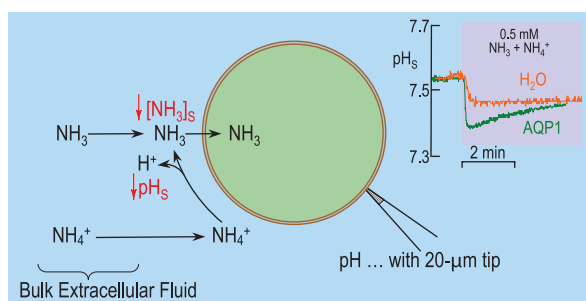


Figure 7. Model of pH_S changes caused by the influx of NH_3 The influx of NH_3 not only causes a rise of pH_i but also a transient fall of pH_S . The two inset pH_S records at the top right come from oocytes injected either with water or with cRNA encoding human AQP1; the same oocytes as in Fig. 6. Data are from Musa-Aziz *et al.* (2009a).

than those of their day-matched controls. Likewise, in response to the application of $\text{NH}_3/\text{NH}_4^+$, AQP1, AmtB and RhAG all produce ΔpH_s values that are significantly larger than those of their day-matched controls. However, AQP4 (Fig. 8E) and AQP5 (Fig. 8F) show no significant permeability to NH_3 . Also, mutations to AmtB (Fig. 8G) and RhAG (Fig. 8H) that are known to render them inactive also reduce $(\Delta\text{pH}_s^*)_{\text{CO}_2}$ and $(\Delta\text{pH}_s^*)_{\text{NH}_3}$ to values that are indistinguishable from those of water-injected oocytes.

Because each oocyte yielded values for $(\Delta\text{pH}_s^*)_{\text{CO}_2}$, $(\Delta\text{pH}_s^*)_{\text{NH}_3}$ and P_f^* , it is possible to get a sense of the relative permeability of each channel to each substance. Figure 9 summarizes the mean channel-specific ΔpH_s values for CO_2 (Fig. 9A) and NH_3 (Fig. 9B) as well as the channel-specific P_f values (Fig. 9C). Note that neither AmtB nor RhAG had any significant water permeability (not shown).

If we now, oocyte by oocyte, divide the $(\Delta\text{pH}_s^*)_{\text{CO}_2}$ value that contributes to Fig. 9A by the P_f^* value that contributes to Fig. 9C, we arrive at a relative index of CO_2 , normalized to the H_2O permeability of the three AQPs (turquoise bars in Fig. 10A). We see that AQP5 has the highest $\text{CO}_2/\text{H}_2\text{O}$ permeability ratio by about a factor of two, with AQP1 and AQP4 following.

Likewise, if we divide the $(\Delta\text{pH}_s^*)_{\text{NH}_3}$ value that contributes to Fig. 9B by the P_f^* value that contributes to Fig. 9C, we arrive at a relative index of NH_3 versus H_2O permeability for the three AQPs (pea-green

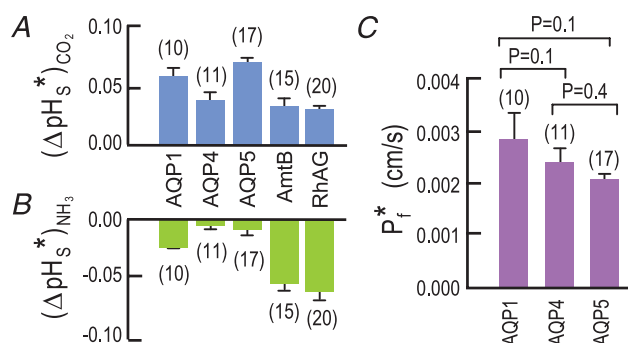


Figure 9. Mean channel-dependent changes in maximal rise of pH_s caused by CO_2 influx (A), maximal fall of pH_s caused by NH_3 influx (B) and osmotic water permeability (C)

The semi-quantitative index of maximal CO_2 flux, $(\Delta\text{pH}_s^*)_{\text{CO}_2}$, is the maximal rise in pH_s (ΔpH_s) in oocytes expressing a channel, less the mean ΔpH_s of day-matched control oocytes (i.e. water-injected oocytes). The semi-quantitative index of maximal NH_3 flux, $(\Delta\text{pH}_s^*)_{\text{NH}_3}$, is the greatest extent of the fall in pH_s (ΔpH_s) in oocytes expressing a channel, less the mean ΔpH_s of day-matched control oocytes (i.e. water-injected oocytes). The value of $(\Delta\text{pH}_s^*)_{\text{NH}_3}$ is not significantly different from zero for either AQP4 or AQP5. P_f^* is the analogous figure for osmotic water permeability. Note that neither AmtB nor RhAG significantly conducted water. Data are from Musa-Aziz *et al.* (2009a).

bars in Fig. 10A). We see that AQP1 has the highest $\text{NH}_3/\text{H}_2\text{O}$ permeability ratio; those for AQP4 and AQP5 are essentially zero because neither has a statistically significant NH_3 permeability. At the other extreme, AmtB

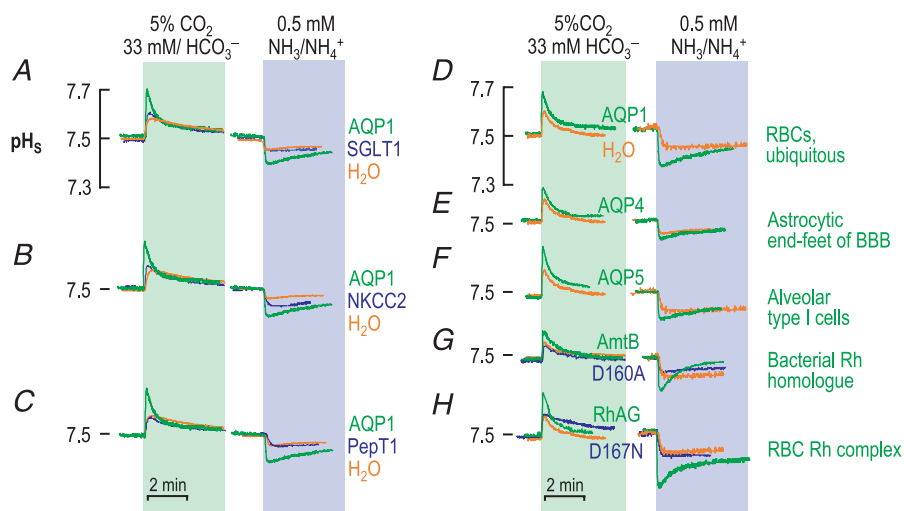


Figure 8. Paired pH_s transients in single oocytes caused by the influx of CO_2 and then the influx of NH_3

Oocytes were injected with either water or cRNA encoding the indicated membrane protein, and then superfused with physiological saline at pH 7.5. The pH_s was monitored as outlined in Figs 6 and 7. For each oocyte, $\text{CO}_2/\text{HCO}_3^-$ was introduced (left half of each panel), washed out (not shown), and then $\text{NH}_3/\text{NH}_4^+$ was introduced (right half of each panel). A–C show that AQP1 but not three transporters can support the pH_s transients. D–H show that AQP1, AQP4, AQP5, AmtB and RhAG can each transport CO_2 , but only AQP1, AmtB and RhAG can transport NH_3 . Data are from Musa-Aziz *et al.* (2009a).

and RhAG, for which the H₂O permeability is negligible, have NH₃/H₂O ratios approaching infinity.

Finally, if we divide the $(\Delta pH_S^*)_{CO_2}$ value that contributes to Fig. 9A by the $(\Delta pH_S^*)_{NH_3}$ value that contributes to Fig. 9B, we arrive at a relative index of CO₂ versus NH₃ permeability for all five channels (Fig. 10B). Since the mean $(\Delta pH_S^*)_{NH_3}$ values for AQP4 and AQP5 do not statistically differ from zero, their ratios are essentially infinity, followed by AQP1, which has a ratio about threefold greater than for AmtB, which in turn has a ratio about twice that of RhAG.

Note that $(\Delta pH_S^*)_{CO_2}$ and $(\Delta pH_S^*)_{NH_3}$ are each semi-quantitative indices of permeability, not permeabilities themselves. Thus, the ratios in Fig. 10 are relative indices of channel permeability, not permeability ratios *per se*. Nevertheless, we obtained all values (and continue to obtain values on other AQPs and Rh proteins) in standard conditions, so that it is meaningful to compare values for the different channels. Ongoing mathematical modelling may eventually yield estimates of absolute permeabilities from pH_S data.

Mechanism of CO₂ and NH₃ permeation through the AQPs and Rh proteins. The data in Figs 8–10 represent the first demonstration of gas selectivity by membrane proteins. An obvious and important question is, ‘What is

the molecular basis for this selectivity?’ Obviously, the size of the transported substance, relative to the size of the pore through which it travels, must be important. However, chemistry must also play a key role. Recall that H₂O and NH₃ have similar dipole moments and that both have tetrahedral electronic structures (compared with H₂O, NH₃ has a proton in place of one lone pair of electrons). Thus, we should not be surprised if sometimes H₂O and NH₃ behave in a similar manner. Carbon dioxide, in contrast, is a linear molecule (O=C=O) with no dipole moment but a quadrupole moment, due to residual negative charge at each oxygen. Thus, CO₂ is much less hydrophilic than H₂O or NH₃. Oxygen, which has no charge separation, is far more hydrophobic.

Regarding the chemistry of the proteins, X-ray structures show that the four monomeric aquapores of AQP1 (Murata *et al.* 2000; Sui *et al.* 2001), for example, have both hydrophilic and hydrophobic surfaces. However, the central pore at the fourfold axis of symmetry is mainly hydrophobic. Molecular dynamic simulations (Tajkhorshid *et al.* 2002) suggest that the H₂O molecules move single file through the aquapore, backing into the pore oxygen-first, flipping orientation near the overlapping asparagine-proline-alanine (NPA) motifs at the centre of the aquapore, and then emerging oxygen-last from the pore. Other molecular dynamic simulations suggest that CO₂ can move single file through an aquapore, interposed between H₂O molecules (Wang *et al.* 2007). However, these simulations predict that CO₂, and particularly O₂, would move far more readily through the central pore. Since, in the absence of dissolved gases, this central pore is predicted not only to be large enough to accept CO₂ but also to be empty (i.e. a vacuum), the central pore could be a highly efficient gas channel. Note that the mobility of CO₂ in the gas phase ($\sim 1.0 \times 10^{-1} \text{ cm}^2 \text{ s}^{-1}$ at 20°C; see Weast, 1978) is about four orders of magnitude greater than through water ($\sim 1.8 \times 10^{-5} \text{ cm}^2 \text{ s}^{-1}$ at 20°C; see Tamimi *et al.* 1994).

The three monomeric NH₃ pores of a homotrimer in the Rh family have a generally hydrophobic character (Khademi *et al.* 2004; Zheng *et al.* 2004; Khademi & Stroud, 2006; Gruswitz *et al.* 2010), but with a conserved antiparallel pair of His residues at the centre. A peculiarity is that the openings to the NH₃ pores are guarded by residues that apparently attract NH₄⁺. Thus, the hypothesized mechanism of transport is that an NH₄⁺ ion from the bulk solution approaches the mouth of the pore and dissociates. The H⁺ would diffuse back into the bulk solution, whereas only the NH₃ would enter the predominantly hydrophobic NH₃ pore. Upon exiting from the opposite end of the pore, the NH₃ would combine with an H⁺ ion (which would diffuse in from the bulk fluid), and the nitrogen would diffuse into the bulk fluid as NH₄⁺.

We have been gaining some insight into the mechanism of gas transport by using inhibitors. Preliminary work

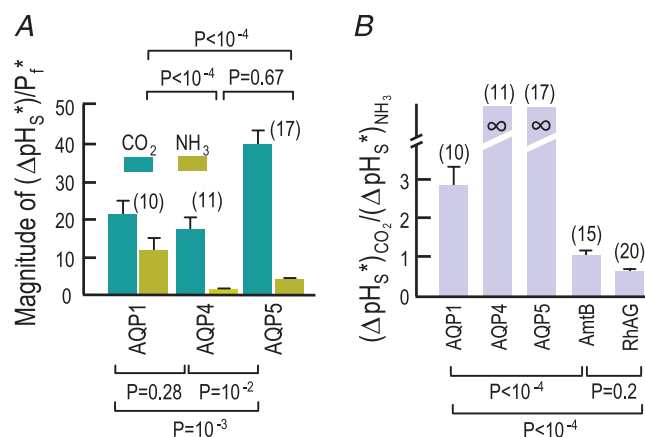


Figure 10. Mean values of $(\Delta pH_S^*)_{CO_2}$ and $(\Delta pH_S^*)_{NH_3}$ normalized to P_{f*} (A) and mean values of $(\Delta pH_S^*)_{CO_2}$ normalized to $(\Delta pH_S^*)_{NH_3}$ (B)

The values in A were obtained by dividing the values of $(\Delta pH_S^*)_{CO_2}$ and $(\Delta pH_S^*)_{NH_3}$ for each oocyte by the value of P_{f*} . These ratios are semi-quantitative indices of CO₂/H₂O permeability ratios and the NH₃/H₂O permeability ratios. The values in B were obtained by dividing the values of $(\Delta pH_S^*)_{CO_2}$ for each oocyte by the value of $(\Delta pH_S^*)_{NH_3}$. These ratios are semi-quantitative indices of CO₂/NH₃ permeability ratios. Since $(\Delta pH_S^*)_{NH_3}$ was not statistically different from zero for AQP4 and AQP5, the NH₃/H₂O ratios for these channels should not be different from zero. Likewise, the CO₂/NH₃ ratios are theoretically infinite. Data are from Musa-Aziz *et al.* (2009a).

by Musa-Aziz and colleagues on AQP1 suggests that the mercurial pCMBS, which is known to inhibit H₂O transport, also reduces (ΔpH_S^*)_{CO₂} by ~40% and eliminates NH₃ permeability (Musa-Aziz *et al.* 2007*a,b*, 2008, 2009*b*). The C189S mutant of AQP1 is immune to these effects of pCMBS. Also with AQP1, we find that DIDS has no effect on either H₂O or NH₃ permeability, but reduces (ΔpH_S^*)_{CO₂} by ~60%. These effects of DIDS persist after scavenging with albumin, consistent with the idea that the DIDS reacts covalently with the AQP1. The DIDS blockade is also unaffected by the C189S mutation. The combination of pCMBS and DIDS reduces (ΔpH_S^*)_{CO₂} by ~100%. Thus, the two inhibitors act on separate pathways that, together, account for all of the CO₂ permeability of AQP1. One pathway, accounting for all H₂O and NH₃ transport, and ~40% of the CO₂, is the monomeric aquapore. Although the other pathway is yet to be established, a reasonable candidate is the central pore.

In the case of AQP4, preliminary data from Musa-Aziz *et al.* (2007*b*) suggest that DIDS blocks nearly all CO₂ permeability, but again none of the H₂O permeability. In the case of AQP5, preliminary work by Musa-Aziz *et al.* (2007*b*) and by Qin & Boron (2010) suggests that DIDS blocks ~75% of the CO₂ permeability, but none of the H₂O permeability. Thus, it is reasonable to suggest that nearly all CO₂, and perhaps O₂ as well, moves through an alternative pathway of these AQPs, perhaps the central pore.

In the cases of AmtB and RhAG, we find that the H₂O permeability is zero (Musa-Aziz *et al.* 2009*a*). Moreover, preliminary work from Musa-Aziz shows that DIDS has no effect on the NH₃ permeability, but blocks virtually all CO₂ permeability. Thus, like the AQPs, the Rh proteins seem to have two distinct pathways for gas transport. One pathway is the monomeric NH₃ pore that conducts NH₃ but apparently not H₂O or substantial amounts of CO₂. The other pathway is the conduit for CO₂, and could be the central pore of the Rh proteins. It will be interesting to see whether O₂ moves through the Rh proteins and, if so, whether it follows the same path as CO₂.

Possible physiological significance of AQPs as gas channels

The first report of a possible physiological role for an AQP as a gas channel came from Uehlein *et al.* (2003), who reported that an AQP in tobacco plants functions as a CO₂ channel and promotes photosynthesis and plant growth.

Roles of AQP1 and Rh complex in RBCs. After the Cl⁻-HCO₃⁻ exchanger AE1, the second and third most abundant integral membrane proteins in the mammalian erythrocyte are AQP1 and the Rh complex. In 2006,

Endeward and colleagues reported work in which they used ¹⁸O-labelled HCO₃⁻ to study the CO₂ permeability of wild-type (WT) *versus* AQP1-null human RBCs (Endeward *et al.* 2006). They found that CO₂ permeability was reduced by ~60% in the AQP1-null RBCs, and that these cells were insensitive to pCMBS. The combination of the absence of AQP1 and the presence of DIDS (which we now appreciate, as noted above, blocks the remnant CO₂ permeability mediated by the Rh complex) reduced CO₂ permeability by ~95%. Thus, at most 5% of the CO₂ could move through the lipid of the plasma membrane.

In 2008, Endeward and colleagues published the complementary work on Rh-null human RBCs (Endeward *et al.* 2008). They found that the absence of the Rh complex reduced the CO₂ permeability by nearly half. This observation supports the conclusion from the previous paragraph; nearly all CO₂ movement through the RBC membrane is mediated by either AE1 or the Rh complex.

In the pulmonary capillary bed, CO₂ comes to diffusion equilibrium between the blood and the alveolar air about one-third of the way along the pulmonary capillary. It is possible that, with the increase in cardiac output that accompanies maximal exercise, the contact time of RBCs with pulmonary capillaries would be sufficiently reduced as to decrease the offloading of CO₂ in the absence of AQP1 and/or the Rh complex, resulting in metabolic acidosis. In principle, the body could compensate by increasing alveolar ventilation, though at the cost of increased work. Another potential role of the channels in RBCs would be as conduits for O₂. During exercise, the absence of the gas channels could lead to a net reduction in O₂ uptake by the end of the pulmonary capillary, causing arterial hypoxaemia, which in turn could limit aerobic exercise.

Effect of AQP1 knockout on exercise. In preliminary work by Xu *et al.* (2010), we have examined voluntary exercise on activity wheels in WT and AQP1-null mice. Wild-type mice that have never seen a wheel typically run 10–12 km day⁻¹ in the absence of any resistance on the wheel. Over a wide range of ambient O₂ levels in the absence of resistance, the distance run by knockout mice is reduced by ~40% compared with WT mice.

Key unanswered questions are whether this exercise deficit is partly overcome by raising ambient [O₂], and whether AQP1 specifically in RBCs plays a role.

Possible role of AQP1 in zebrafish swimbladder. We recently cloned AQP1a from zebrafish (Chen *et al.* 2010), finding that the protein is most highly expressed in RBCs, the swimbladder, and in regions of the avascular retina that correspond to the portions of the photoreceptor cell that contains mitochondria.

During the period immediately after making the transition from embryo to larva, the zebrafish has poorly

developed gills, and inflates its swimbladder (connected to the oesophagus by a pneumatic duct) by gulping air. In unpublished work, Nick Courtney finds that if he replaces room air with 100% N₂ between 3 and 10 days postfertilization, then at day 10, the '100% N₂' fish have a dry mass that is ~25% less than their room-air littermates. These data are consistent with the hypothesis that, at least during this part of the zebrafish life, the swimbladder functions as a respiratory organ. We are extending these experiments to several combinations of [O₂] in the water and gas phases, and hope to be able to repeat the work with AQP1a-null zebrafish.

Role of AQP1 in HCO₃⁻ reabsorption by the renal proximal tubule. One of the major tasks of the renal proximal tubule (PT) is to reabsorb (i.e. to move from lumen to blood) ~80% of the HCO₃⁻ filtered at the glomerulus. More distal portions of the nephron reabsorb the remainder of the filtered HCO₃⁻. As outlined in Fig. 11, the cells of the PT secrete H⁺ into the tubule lumen using both the Na⁺-H⁺ exchanger NHE3 and a vacuolar-type H⁺ pump at the apical membrane. Once in the lumen, the H⁺ titrates HCO₃⁻ to form H₂O and CO₂, catalysed by carbonic anhydrase IV (CAIV), which is linked to the apical membrane. The secreted H⁺ also titrates weak bases other than HCO₃⁻, such as NH₃ and inorganic phosphate. The titration of these other weak bases removes from the body the H⁺ that accumulates in the body as the result of metabolism and the ingestion of acidic foodstuffs. The newly formed CO₂ and H₂O enter the cell, where they recombine to form H⁺ and HCO₃⁻, catalysed by the soluble enzyme CAII. The cell exports the H⁺ across the apical membrane to the lumen as noted above, and uses the electrogenic Na⁺-HCO₃⁻ cotransporter NBCe1-A to move the HCO₃⁻ across the basolateral membrane and into the interstitial space, which is in contact with the blood.

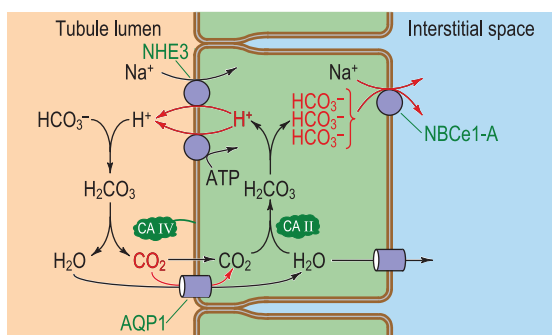


Figure 11. Model of HCO₃⁻ reabsorption by the renal proximal tubule

Bicarbonate appears in the lumen of the proximal tubule as the result of glomerular filtration. Abbreviations: AQP1, aquaporin 1; CAII, carbonic anhydrase II; CAIV, carbonic anhydrase IV; NBCe1-A, renal splice variant of electrogenic Na/HCO₃ cotransporter 1; and NHE3, Na⁺-H⁺ exchanger 3.

Let us return now to the H₂O and CO₂ formed in the lumen. The vast majority of the reabsorbed H₂O moves across the apical and basolateral membranes through AQP1 (Schnermann *et al.* 1998; Vallon *et al.* 2000). Preliminary data by Zhou *et al.* (2006) show that the maximal HCO₃⁻ reabsorption rate is reduced by ~60% in PTs from AQP1-null mice compared with WT mice. Alan Verkman generously provided the AQP1-null mice. In additional experiments, Zhao *et al.* (1995) perfused the tubule lumen with a CO₂/HCO₃⁻-free solution and then used out-of-equilibrium solution technology to present to the basolateral solution either HCO₃⁻ in the absence of CO₂ or CO₂ in the absence of HCO₃⁻, always at pH 7.40. They found that with only HCO₃⁻ in the bath, the 'carbon backflux' from bath to lumen was identical in AQP1-null *versus* WT tubules (Zhou *et al.* 2006). However, with only CO₂ in the bath, the 'carbon backflux' from bath to lumen was ~60% lower in AQP1-null *versus* WT tubules. Thus, AQP1 seems to be required for ~60% of the transepithelial CO₂ permeability of the PT.

If this AQP1-dependent CO₂ permeability is physiologically important, we might predict that AQP1-null mice distal nephron segments, in the absence of a challenge to their acid-base status, would compensate for the deficit in PT function, and that the AQP1-null mice would have a more-or-less normal arterial pH. However, we might also predict that in the face of a chronic metabolic or respiratory acidosis, the AQP1-null mice would be unable to adapt further, and thus would exhibit a low arterial pH relative to WT mice.

Scrutiny

The gas-channel hypothesis, if correct and if it proves to be physiologically important, would represent a major paradigm shift. Thus, it is healthy that this emerging paradigm be held up to close examination.

A view from stopped-flow and mice. An early analysis of the gas-channel hypothesis revolved around the following three types of experiments (Yang *et al.* 2000; Fang *et al.* 2002): (1) stopped-flow analysis of WT *versus* AQP1-null RBCs; (2) stopped-flow analysis of liposomes with or without reconstituted AQP1; and (3) the uptake of CO₂ by artificially ventilated lungs of WT *versus* AQP1-null mice. As previously discussed (Cooper *et al.* 2002), the RBC stopped-flow experiments yielded values for CO₂ permeability that were at least one order of magnitude smaller than those of earlier workers, and was probably due to inadequate mixing in the stopped-flow apparatus, generating large unstirred layers. This same limitation probably applied to the liposomes. In both cases, it would have been difficult to detect the CO₂ permeability of AQP1. In the mouse-lung experiments (no doubt a technical

feat), the introduction of CO₂ into the inspired air led to the expected increase in arterial partial pressure of CO₂. However, the half-time for the rise in arterial CO₂ partial pressure (~2 min) was far slower than what we would have expected for the wash-in of CO₂ into the alveoli. Thus, it would have been difficult to detect an effect of AQP1 on CO₂ permeability.

A view from artificial bilayers. More recently, in a series of physical chemistry papers by Missner and colleagues (Missner *et al.* 2008*a,b*; Missner & Pohl, 2009), the authors, who studied artificial planar lipid bilayers, concluded that ‘Overton continues to rule’. Their twofold argument, in brief, is as follows. (1) The unstirred layers enveloping a membrane are so large that their aggregate resistance dominates the macroscopic resistance to the diffusion of a substance such as CO₂ from one bulk aqueous solution, through the membrane, to another bulk aqueous solution. Stated somewhat differently, the resistance offered by the membrane is simply too small to be significant. (2) The membrane lipid has such a high gas (e.g. CO₂) permeability that the presence of a protein channel could not enhance the flux. My sense is that the aforementioned experimental work of Missner and colleagues is basically correct, as are the conclusions that narrowly flow from that work. Where we differ is on the application of general principles to real biological membranes; problems of series and parallel resistances.

We have already introduced the importance of unstirred layers, which represent a resistance to diffusion in series with the membrane lipid (see section ‘Overton’s rule’). If one were to set up experimental conditions with increasingly large unstirred layers, it would become increasingly difficult to detect the contribution of the membrane. One could compound matters by choosing a membrane with a low baseline resistance to gas diffusion. This is the situation that prevails when working with planar artificial lipid bilayers: large unstirred layers (100–200 μm) and membranes composed only of lipids and, at that, lipids with high intrinsic permeabilities to gases such as CO₂. In such a system, the membrane makes an insignificant contribution to macroscopic CO₂ resistance, independent of the presence of gas channels or the validity of Overton’s rule. This is the problem of the series resistance. It will be difficult for the experimenter to detect the action of gas channels unless the unstirred layers are sufficiently small relative to the resistance of the membrane with or without the channel. Since biological unstirred layers are generally tiny where they count (e.g. surrounding the RBC membrane, from alveolar air to pulmonary capillary blood), the series resistance is not a problem for physiology, but rather for physiologists trying to make measurements.

Even if one were to reduce the aggregate unstirred layer by a couple orders of magnitude to mimic the

conditions faced, for example, by mammalian RBCs or the proximal-tubule apical membrane, gas channels could not enhance permeability if embedded in a sea of highly permeable lipid. Indeed, as noted by Tajkhorshid and colleagues (Wang *et al.* 2007), molecular-dynamics modelling suggests that introducing AQP1, or presumably any protein, into a membrane made of palmitoyl-oleoyl-phosphatidylethanolamine would decrease overall membrane permeability owing to the high permeability of the lipid *per se*. This is the problem of parallel resistance. A gas channel cannot enhance permeability unless the lipid surrounding the channel is relatively tight.

Thus, in order for a gas channel to enhance the permeability of a membrane to CO₂, ignoring unstirred layers, the surrounding lipid must be exceptionally tight. I suspect that this is almost never the case in artificial systems, and it may not be the rule even in living organisms. Thus, even though Overton’s rule is overly simplistic from a biophysics perspective, the classical notion that gases diffuse through the lipid phase of the membrane is probably valid for many cell membranes, but not all.

Where might gas channels make sense? As outlined previously (Cooper *et al.* 2002) they might make sense in the following conditions.

- When the background or intrinsic permeability of the membrane lipid is low. This is a *sine qua non*, which is why I devoted attention to the access-solubility-diffusion-protein-egress hypothesis. Several biological membranes probably fit the bill. Candidates might include any membrane that faces a physical or chemical environment that is sufficiently hostile as to require a robust membrane. Erythrocytes and *Xenopus* oocytes come to mind. Perhaps the quintessential membranes in this regard are the ones that got us thinking outside the box about gas transport in the first place, the apical membranes of gastric glands, but these certainly lack gas channels. Another fertile recruiting ground might be membranes that are required to withstand large chemical or electrical gradients. Apical membranes of certain epithelia (e.g. renal collecting ducts) and the mitochondrial inner membrane are possibilities.
- When the gas gradient is small. Examples might be the influx of CO₂ from air (0.03% CO₂) into plant cells, or from tissues into systemic capillaries.
- When the required gas flux is high. Examples would be the alveolar–capillary barrier in the lung, the RBC membrane and the apical membrane of proximal tubules.

The second and third bullet points merely restate eqn (5).

One conclusion to be drawn from the above analysis is that those wishing to study gas channels must use an experimental system that has a favourable combination of small unstirred layers, a low background permeability of membrane lipids and a high expression level of the channel. There are no absolutes; one can overcome the disadvantages of a somewhat larger unstirred layer if the intrinsic permeability of the membrane is sufficiently low, as seems to be the case in the *Xenopus* oocyte.

Concluding remarks

Long before the first evidence for gas movement through channels, the discovery of water channels represented a major milestone in membrane biology. Moreover, certain members of the AQP family can, in addition to water, transport small organic molecules, such as glycerol and urea (Murata *et al.* 2000; Sui *et al.* 2001). If gas transport through the AQPs proves to be physiologically relevant, this fact would further underscore the importance of the AQP family.

One should not view H₂O and CO₂ movement through AQP1, AQP4 or AQP5 as an either–or issue, although one could imagine that a cell could independently gate the monomeric aquapores and the alternative CO₂ pathway (e.g. central pore). If we will ignore this possibility for the moment, then (if gas permeation proves to be physiologically important) the major physiological contribution of an AQP would depend on its anatomical context.

At one extreme, AQP2 in the renal collecting duct, for example, might conduct CO₂, but presumably that function would be of minor significance compared with the impact on water homeostasis.

At the other extreme, it is not clear why the H₂O permeability *per se* of AQP1 confers an advantage in the mission of an erythrocyte, which has evolved to carry CO₂ and O₂ efficiently. On the contrary, it is possible that a high RBC H₂O permeability would render the cell vulnerable to rapid shrinkage as the RBC flows deep into the hypertonic renal medulla. Perhaps this selective pressure led to the presence of urea transporters to reduce the reflection coefficient and thereby minimize volume changes.

In the middle of this spectrum might be AQP1 in the apical membrane of the renal proximal tubule. Here the AQP1 is necessary for the high H₂O permeability that allows the PT to reabsorb large volumes of essentially isotonic saline. However, the AQP1 also appears to be responsible for 60% of the CO₂ permeability that is necessary for HCO₃⁻ reabsorption.

In the brain, the membrane of the astrocytic end-feet that envelop blood vessels contains semi-crystalline arrays of AQP4 that occupy about one-third of the total

membrane surface area. Knocking out the AQP4 reduces the osmotic water permeability of the blood–brain barrier by ~90% and renders the mice more resistant to the cerebral oedema that occurs following a model of stroke (Manley *et al.* 2000). Might AQP4 contribute to the CO₂ flux across the blood–brain barrier? It is interesting to recall that AQP4 has a negligible permeability to NH₃, which is neurotoxic.

In principle, AQP5 in the lung could serve as a pathway for CO₂ across the apical membranes of the type I alveolar pneumocytes.

The discovery that the Rh proteins conduct NH₃ and CO₂ provides a function for the erythroid Rh complex that heretofore has had only a pathological role.

Finally, what advantages might gas channels provide?

- When the background gas permeability of a membrane is low, channels would enhance flux.
- Channels would allow cells to display selectivity for particular gases.
- Channels would allow cells to regulate gas permeability.
- Although not an advantage to the cell *per se*, an advantage to the scientist or physician is that gas channels could make gas permeability amenable to selective pharmacological intervention.

Thus far, the only gases of relevance to mammals that have been studied in the context of gas channels are CO₂, NH₃ and NO. Conspicuous by its absence from this list is O₂. Moving forward, it will be important to make progress on the following four fronts: (1) extending the work to O₂ as well as CO, N₂ and other gases; (2) understanding the molecular mechanism of gas transport and selectivity by AQP and Rh channels; (3) determining whether cells can gate or otherwise regulate gas channels; and (4) testing the physiological relevance of gas transport through channels.

References

- Aickin CC & Thomas RC (1977). An investigation of the ionic mechanism of intracellular pH regulation in mouse soleus muscle fibres. *J Physiol* **273**, 295–316.
- Amiry-Moghaddam M, Frydenlund DS & Ottersen OP (2004). Anchoring of aquaporin-4 in brain: molecular mechanisms and implications for the physiology and pathophysiology of water transport. *Neuroscience* **129**, 999–1010.
- Andrade SL, Dickmanns A, Ficner R & Einsle O (2005). Crystal structure of the archaeal ammonium transporter Amt-1 from *Archaeoglobus fulgidus*. *Proc Natl Acad Sci USA* **102**, 14994–14999.
- Bakouh N, Benjelloun F, Cherif-Zahar B & Planelles G (2006). The challenge of understanding ammonium homeostasis and the role of the Rh glycoproteins. *Transfus Clin Biol* **13**, 139–146.

- Bevensee MO & Boron WF (2008). Regulation of intracellular pH. In *Seldin and Giebisch's The Kidney: Physiology and Pathophysiology*, ed. Alpern RJ & Hebert SC, pp. 1429–1480. Academic Press, Burlington, MA.
- Biver S, Belge H, Bourgeois S, Van Vooren P, Nowik M, Scohy S, Houillier P, Szpirer J, Szpirer C, Wagner CA, Devuyst O & Marini AM (2008). A role for Rhesus factor Rhcg in renal ammonium excretion and male fertility. *Nature* **456**, 339–343.
- Blank M & Roughton FJW (1960). The permeability of monolayers to carbon dioxide. *Trans Faraday Soc* **56**, 1832–1841.
- Boron WF (1977). Intracellular pH transients in giant barnacle muscle fibers. *Am J Physiol* **233**, C61–C73.
- Boron WF (2004). Regulation of intracellular pH. *Adv Physiol Educ* **28**, 160–179.
- Boron WF & Boulpaep EL (eds) (2009). *Medical Physiology. A Cellular and Molecular Approach*, 2nd edn, 1337 pp. Saunders Elsevier, Philadelphia.
- Boron WF & Cooper GJ (1998). Effect of DIDS on the CO₂ permeability of the water channel AQP1. *FASEB J* **12**, A374.
- Boron WF & De Weer P (1976a). Active proton transport stimulated by CO₂/HCO₃⁻ blocked by cyanide. *Nature* **259**, 240–241.
- Boron WF & De Weer P (1976b). Intracellular pH transients in squid giant axons caused by CO₂, NH₃ and metabolic inhibitors. *J Gen Physiol* **67**, 91–112.
- Boron WF & Russell JM (1983). Stoichiometry and ion dependencies of the intracellular-pH-regulating mechanism in squid giant axons. *J Gen Physiol* **81**, 373–399.
- Burckhardt BC & Frömter E (1992). Pathways of NH₃/NH₄⁺ permeation across *Xenopus laevis* oocyte cell membrane. *Pflügers Arch* **420**, 83–86.
- Burg M, Grantham J, Abramow M & Orloff J (1966). Preparation and study of fragments of single rabbit nephrons. *Am J Physiol* **210**, 1293–1298.
- Caldwell PC (1958). Studies on the internal pH of large muscle and nerve fibres. *J Physiol* **142**, 22–62.
- Casey JR, Grinstein S & Orlowski J (2010). Sensors and regulators of intracellular pH. *Nat Rev Mol Cell Biol* **11**, 50–61.
- Chen LM, Zhao J, Musa-Aziz R, Pelletier MF, Drummond IA & Boron WF (2010). Cloning and characterization of a zebrafish homologue of human AQP1: a bifunctional water and gas channel. *Am J Physiol Regul Integr Comp Physiol*, doi: 10.1152/ajpregu.00319.2010.
- Chesler M (1986). Regulation of intracellular pH in reticulospinal neurones of the lamprey, *Petromyzon marinus*. *J Physiol* **381**, 241–261.
- Colin Y, Chérif-Zahar B, Vankim CL, Raynal V, Vanhuffel V & Cartron JP (1991). Genetic basis of the Rhd-positive and Rhd-negative blood-group polymorphism as determined by Southern analysis. *Blood* **78**, 2747–2752.
- Conroy MJ, Durand A, Lupo D, Li XD, Bullough PA, Winkler FK & Merrick M (2007). The crystal structure of the *Escherichia coli* AmtB–GlnK complex reveals how GlnK regulates the ammonia channel. *Proc Natl Acad Sci USA* **104**, 1213–1218.
- Cooper GJ & Boron WF (1998). Effect of PCMBs on CO₂ permeability of *Xenopus* oocytes expressing aquaporin 1 or its C189S mutant. *Am J Physiol Cell Physiol* **275**, C1481–C1486.
- Cooper GJ, Zhou Y, Bouyer P, Grichtchenko II & Boron WF (2002). Transport of volatile solutes through AQP1. *J Physiol* **542**, 17–29.
- De Hemptinne A & Huguenin F (1984). The influence of muscle respiration and glycolysis on surface and intracellular pH in fibres of the rat soleus. *J Physiol* **347**, 581–592.
- Denker BM, Smith BL, Kuhajda FP & Agre P (1988). Identification, purification, and partial characterization of a novel M_r 28,000 integral membrane protein from erythrocytes and renal tubules. *J Biol Chem* **263**, 15634–15642.
- Eladari D, Cheval L, Quentin F, Bertrand O, Mouro I, Chérif-Zahar B, Cartron JP, Paillard M, Doucet A & Chambrey R (2002). Expression of RhCG, a new putative NH₃/NH₄⁺ transporter, along the rat nephron. *J Am Soc Nephrol* **13**, 1999–2008.
- Endeward V, Cartron JP, Ripoché P & Gros G (2008). RhAG protein of the Rhesus complex is a CO₂ channel in the human red cell membrane. *FASEB J* **22**, 64–73.
- Endeward V, Musa-Aziz R, Cooper GJ, Chen L, Pelletier MF, Virkki LV, Supuran CT, King LS, Boron WS & Gros G (2006). Evidence that aquaporin 1 is a major pathway for CO₂ transport across the human erythrocyte membrane. *FASEB J* **20**, 1974–1981.
- Engelman DM (2005). Membranes are more mosaic than fluid. *Nature* **438**, 578–580.
- Eyers SA, Ridgwell K, Mawby WJ & Tanner MJ (1994). Topology and organization of human Rh (rhesus) blood group-related polypeptides. *J Biol Chem* **269**, 6417–6423.
- Fabiny JM, Jayakumar A, Chinault AC & Barnes EM Jr (1991). Ammonium transport in *Escherichia coli*: localization and nucleotide sequence of the *amtA* gene. *J Gen Microbiol* **137**, 983–989.
- Fang X, Yang B, Matthay MA & Verkman AS (2002). Evidence against aquaporin-1-dependent CO₂ permeability in lung and kidney of mice. *J Physiol* **542**, 63–69.
- Fenn WO & Cobb DM (1934). The potassium equilibrium in muscle. *J Gen Physiol* **17**, 629–656.
- Fenn WO & Maurer FW (1935). The pH of muscle. *Protoplasma* **24**, 337–345.
- Finkelstein A (1986). *Water Movement Through Lipid Bilayers, Pores, and Plasma Membranes. Theory and Reality*. John Wiley & Sons, New York.
- Forster RE, Gros G, Lin L, Ono Y & Wunder M (1998). The effect of 4,4'-diisothiocyanato-stilbene-2,2'-disulfonate on CO₂ permeability of the red blood cell membrane. *Proc Natl Acad Sci USA* **95**, 15815–15820.
- Garvin JL, Burg MB & Knepper MA (1988). Active NH₄⁺ absorption by the thick ascending limb. *Am J Physiol Renal Physiol* **255**, F57–F65.
- Gruswitz F, Chaudhary S, Ho JD, Schlessinger A, Pezeshki B, Ho CM, Sali A, Westhoff CM & Stroud RM (2010). Function of human Rh based on structure of RhCG at 2.1 Å. *Proc Natl Acad Sci USA* **107**, 9638–9643.

- Gutknecht J, Bisson MA & Tosteson FC (1977). Diffusion of carbon dioxide through lipid bilayer membranes. *J Gen Physiol* **69**, 779–794.
- Hamm LL, Trigg D, Martin D, Gillespie C & Buerkert J (1985). Transport of ammonia in the rabbit cortical collecting tubule. *J Clin Invest* **75**, 478–485.
- Han KH, Croker BP, Clapp WL, Werner D, Sahni M, Kim J, Kim HY, Handlogten ME & Weiner ID (2006). Expression of the ammonia transporter, RhC glycoprotein, in normal and neoplastic human kidney. *J Am Soc Nephrol* **17**, 2670–2679.
- Han KH, Mekala K, Babida V, Kim HY, Handlogten ME, Verlander JW & Weiner ID (2009). Expression of the gas-transporting proteins, Rh B glycoprotein and Rh C glycoprotein, in the murine lung. *Am J Physiol Lung Cell Mol Physiol* **297**, L153–L163.
- Handlogten ME, Hong SP, Zhang L, Vander AW, Steinbaum ML, Campbell-Thompson M & Weiner ID (2005). Expression of the ammonia transporter proteins Rh B glycoprotein and Rh C glycoprotein in the intestinal tract. *Am J Physiol Gastrointest Liver Physiol* **288**, G1036–G1047.
- Harvey EN (1911). Studies on the permeability of cells. *J Exp Zool* **10**, 507–556.
- Herrera M & Garvin JL (2007). Novel role of AQP-1 in NO-dependent vasorelaxation. *Am J Physiol Renal Physiol* **292**, F1443–F1451.
- Herrera M, Hong NJ & Garvin JL (2006). Aquaporin-1 transports NO across cell membranes. *Hypertension* **48**, 157–164.
- Hill L (1935). Sir Edward Albert Sharpey-Schafer 1850–1935. *Obituary Notices of the Fellows of the Royal Society* **1**, 401–407.
- Jacobs MH (1920). To what extent are the physiological effects of carbon dioxide due to hydrogen ions? *Am J Physiol* **51**, 321–331.
- Jacobs MH (1922). The influence of ammonium salts on cell reaction. *J Gen Physiol* **5**, 181–188.
- Kawasaki K, Yin JJ, Subczynski WK, Hyde JS & Kusumi A (2001). Pulse EPR detection of lipid exchange between protein-rich raft and bulk domains in the membrane: methodology development and its application to studies of influenza viral membrane. *Biophys J* **80**, 738–748.
- Keicher E & Meech R (1994). Endogenous Na⁺–K⁺ (or NH₄⁺)–2Cl[–] cotransport in *Rana* oocytes; anomalous effect of external NH₄⁺ on pHi. *J Physiol* **475**, 45–57.
- Khademi S, O'Connell J 3rd, Remis J, Robles-Colmenares Y, Miericke LJW & Stroud RM (2004). Mechanism of ammonia transport by Amt/MEP/Rh: structure of AmtB at 1.35 Å. *Science* **305**, 1587–1594.
- Khademi S & Stroud RM (2006). The Amt/MEP/Rh family: Structure of AmtB and the mechanism of ammonia gas conduction. *Physiology (Bethesda)* **21**, 419–429.
- Kikeri D, Sun A, Zeidel ML & Hebert SC (1989). Cell membranes impermeable to NH₃. *Nature* **339**, 478–480.
- Kim HY, Verlander JW, Bishop JM, Cain BD, Han KH, Igarashi P, Lee HW, Handlogten ME & Weiner ID (2009). Basolateral expression of the ammonia transporter family member Rh C glycoprotein in the mouse kidney. *Am J Physiol Renal Physiol* **296**, F543–F555.
- Kinne R, Kinne-Saffran E, Schutz H & Scholermann B (1986). Ammonium transport in medullary thick ascending limb of rabbit kidney: involvement of the Na⁺, K⁺, Cl[–] cotransporter. *J Membr Biol* **94**, 279–284.
- Lee HW, Verlander JW, Bishop JM, Igarashi P, Handlogten ME & Weiner ID (2009). Collecting duct-specific Rh C glycoprotein deletion alters basal and acidosis-stimulated renal ammonia excretion. *Am J Physiol Renal Physiol* **296**, F1364–F1375.
- Lee HW, Verlander JW, Bishop JM, Nelson RD, Handlogten ME & Weiner ID (2010). Effect of intercalated cell-specific Rh C glycoprotein deletion on basal and metabolic acidosis-stimulated renal ammonia excretion. *Am J Physiol Renal Physiol* **299**, F369–F379.
- Leventis PA & Grinstein S (2010). The distribution and function of phosphatidylserine in cellular membranes. *Annu Rev Biophys* **39**, 407–427.
- Liu Z, Chen Y, Mo R, Hui C, Cheng JF, Mohandas N & Huang CH (2000). Characterization of human RhCG and mouse Rhcg as novel nonerythroid Rh glycoprotein homologues predominantly expressed in kidney and testis. *J Biol Chem* **275**, 25641–25651.
- Liu Z, Peng J, Mo R, Hui C & Huang CH (2001). Rh type B glycoprotein is a new member of the Rh superfamily and a putative ammonia transporter in mammals. *J Biol Chem* **276**, 1424–1433.
- Lupo D, Li XD, Durand A, Tomizaki T, Cherif-Zahar B, Matassi G, Merrick M & Winkler FK (2007). The 1.3-Å resolution structure of *Nitrosomonas europaea* Rh50 and mechanistic implications for NH₃ transport by Rhesus family proteins. *Proc Natl Acad Sci USA* **104**, 19303–19308.
- Macey RI (1984). Transport of water and urea in red blood cells. *Am J Physiol Cell Physiol* **246**, C195–C203.
- Manley GT, Fujimura M, Ma T, Noshita N, Filiz F, Bollen AW, Chan P & Verkman AS (2000). Aquaporin-4 deletion in mice reduces brain edema after acute water intoxication and ischemic stroke. *Nat Med* **6**, 159–163.
- Marini AM, Matassi G, Raynal V, André B, Cartron JP & Chérif-Zahar B (2000). The human Rhesus-associated RhAG protein and a kidney homologue promote ammonium transport in yeast. *Nat Genet* **26**, 341–344.
- Marini AM, Urrestarazu A, Beauwens R & André B (1997). The Rh (rhesus) blood group polypeptides are related to NH₄⁺ transporters. *Trends Biochem Sci* **22**, 460–461.
- Marini AM, Vissers S, Urrestarazu A & André B (1994). Cloning and expression of the *MEP1* gene encoding an ammonium transporter in *Saccharomyces cerevisiae*. *EMBO J* **13**, 3456–3463.
- Missner A, Kügler P, Antonenko YN & Pohl P (2008a). Passive transport across bilayer lipid membranes: Overton continues to rule. *Proc Natl Acad Sci USA* **105**, E123.
- Missner A, Kügler P, Saparov SM, Sommer K, Mathai JC, Zeidel ML & Pohl P (2008b). Carbon dioxide transport through membranes. *J Biol Chem* **283**, 25340–25347.
- Missner A & Pohl P (2009). 110 Years of the Meyer–Overton rule: predicting membrane permeability of gases and other small compounds. *Chemphyschem* **10**, 1405–1414.
- Murata K, Mitsuoka K, Hirai T, Walz T, Agre P, Heymann JB, Engel A & Fujiyoshi Y (2000). Structural determinants of water permeation through aquaporin-1. *Nature* **407**, 599–605.

- Murer H, Hopfer U & Kinne R (1976). Sodium/proton antiport in brush-border-membrane vesicles isolated from rat small intestine and kidney. *Biochem J* **154**, 597–604.
- Musa-Aziz R, Chen L, Pelletier MF & Boron WF (2009a). Relative CO₂/NH₃ selectivities of AQP1, AQP4, AQP5, AmtB, and RhAG. *Proc Natl Acad Sci USA* **106**, 5406–5411.
- Musa-Aziz R, Chen LM & Boron WF (2007a). Differential effects of DIDS on the CO₂ vs NH₃ permeability of AQP1, AmtB, and RhAG. *International Society of Nephrology, Rio de Janeiro, Brazil, 2007*.
- Musa-Aziz R, Chen LM & Boron WF (2007b). The CO₂/NH₃ selectivity of AQP1, AQP4, and AQP5 and now it is affected by DIDS. *J Am Soc Nephrol* **18**, 6A.
- Musa-Aziz R, Geyer RR, Shaikh S, Tajkhorshid E & Boron WF (2009b). Investigating the mechanism of CO₂ transport through human AQP1. *J Am Soc Nephrol* **20**, 34A.
- Musa-Aziz R, Jiang L, Chen LM, Behar KL & Boron WF (2009c). Concentration-dependent effects on intracellular and surface pH of exposing *Xenopus* oocytes to solutions containing NH₃/NH₄⁺. *J Membr Biol* **228**, 15–31.
- Musa-Aziz R, Pergher P & Boron WF (2008). Evidence from surface-pH transients that DIDS and pCMBS reduce the CO₂ permeability of AQP1 expressed in *Xenopus* oocytes. *J Am Soc Nephrol* **19**, 350A.
- Nakhoul NL, Davis BA, Romero MF & Boron WF (1998). Effect of expressing the water channel aquaporin-1 on the CO₂ permeability of *Xenopus* oocytes. *Am J Physiol Cell Physiol* **274**, C543–C548.
- Nakhoul NL & Hamm LL (2004). Non-erythroid Rh glycoproteins: a putative new family of mammalian ammonium transporters. *Pflügers Arch* **447**, 807–812.
- Oliver G & Schafer EA (1895). The physiological effects of extracts of the suprarenal capsules. *J Physiol* **18**, 230–276.
- Overton E (1897). Über die osmotischen Eigenschaften der Zelle in ihrer Bedeutung für die Toxicologie und Pharmacologie. *Z Phys Chem* **22**, 189–209.
- Prasad GV, Coury LA, Fin F & Zeidel ML (1998). Reconstituted aquaporin 1 water channels transport CO₂ across membranes. *J Biol Chem* **273**, 33123–33126.
- Preston GM & Agre P (1991). Isolation of the cDNA for erythrocyte integral membrane protein of 28 kilodaltons: member of an ancient channel family. *Proc Natl Acad Sci USA* **88**, 11110–11114.
- Preston GM, Carroll TP, Guggino WB & Agre P (1992). Appearance of water channels in *Xenopus* oocytes expressing red cell CHIP28 protein. *Science* **256**, 385–387.
- Preston GM, Jung JS, Guggino WB & Agre P (1993). The mercury-sensitive residue at cysteine 189 in the CHIP28 water channel. *J Biol Chem* **268**, 17–20.
- Qin X & Boron WF (2010). Effect of DIDS and pCMBS on the CO₂ permeability of human aquaporin-5 (AQP5). *FASEB J* **24**, 610.5.
- Quentin F, Eladari D, Cheval L, Lopez C, Goossens D, Colin Y, Cartron JP, Paillard M & Chambrey R (2003). RhBG and RhCG, the putative ammonia transporters, are expressed in the same cells in the distal nephron. *J Am Soc Nephrol* **14**, 545–554.
- Ripoche P, Bertrand O, Gane P, Birkenmeier C, Colin Y & Cartron JP (2004). Human Rhesus-associated glycoprotein mediates facilitated transport of NH₃ into red blood cells. *Proc Natl Acad Sci USA* **101**, 17222–17227.
- Ripoche P, Goossens D, Devuyst O, Gane P, Colin Y, Verkman AS & Cartron JP (2006). Role of RhAG and AQP1 in NH₃ and CO₂ gas transport in red cell ghosts: a stopped-flow analysis. *Transfus Clin Biol* **13**, 117–122.
- Roos A (1975). Intracellular pH and distribution of weak acids across cell membranes. A study of D- and L-lactate and of DMO in rat diaphragm. *J Physiol* **249**, 1–25.
- Roos A & Boron WF (1981). Intracellular pH. *Physiol Rev* **61**, 296–434.
- Russell JM & Boron WF (1976). Role of chloride transport in regulation of intracellular pH. *Nature* **264**, 73–74.
- Schnermann J, Chou CL, Ma T, Traynor T, Knepper MA & Verkman AS (1998). Defective proximal tubular fluid reabsorption in transgenic aquaporin-1 null mice. *Proc Natl Acad Sci USA* **95**, 9660–9664.
- Seshadri RM, Klein JD, Kozlowski S, Sands JM, Kim YH, Han KH, Handlogten ME, Verlander JW & Weiner ID (2006). Renal expression of the ammonia transporters, Rhbg and Rhcg, in response to chronic metabolic acidosis. *Am J Physiol Renal Physiol* **290**, F397–F408.
- Anon (1963). E. P. Sharpey-Schafer, F.R.C.P. *BMJ* **2**, 1135–1136.
- Simon SA & Gutknecht J (1980). Solubility of carbon dioxide in lipid bilayer membranes and organic solvents. *Biochim Biophys Acta* **596**, 352–358.
- Singh SK, Binder HJ, Geibel JP & Boron WF (1995). An apical permeability barrier to NH₃/NH₄⁺ in isolated, perfused colonic crypts. *Proc Natl Acad Sci USA* **92**, 11573–11577.
- Stannett V (1978). The transport of gases in synthetic polymeric membranes – an historic perspective. *J Membr Sci* **3**, 97–115.
- Subczynski WK & Swartz HM (2005). EPR oximetry in biological and model samples. In *Biomedical EPR-Part A: Free Radicals, Metals, Medicine, and Physiology*, ed. Eaton SR, Eaton GR & Berliner LJ, pp. 229–282. Kluwer, New York.
- Subczynski WK, Widomska J & Feix JB (2009). Physical properties of lipid bilayers from EPR spin labeling and their influence on chemical reactions in a membrane environment. *Free Radic Biol Med* **46**, 707–718.
- Sui H, Han BG, Lee JK, Walian P & Jap BK (2001). Structural basis of water-specific transport through the AQP1 water channel. *Nature* **414**, 872–878.
- Tajkhorshid E, Nollert P, Jensen MØ, Miercke LJ, O’Connell J, Stroud RM, Schulten K (2002). Control of the selectivity of the aquaporin water channel family by global orientational tuning. *Science* **296**, 525–530.
- Takamori S, Holt M, Stenius K, Lemke EA, Grønborg M, Riedel D et al. (2006). Molecular anatomy of a trafficking organelle. *Cell* **127**, 831–846.
- Tamimi A, Rinker EB & Sandall OC (1994). Diffusion coefficients for hydrogen sulfide, carbon dioxide, and nitrous oxide in water over the temperature range 293–368K. *J Chem Eng Data* **39**, 330–332.
- Thomas RC (1974). Intracellular pH of snail neurones measured with a new pH-sensitive glass micro-electrode. *J Physiol* **238**, 159–180.
- Thomas RC (1976). Ionic mechanism of the H⁺ pump in a snail neurone. *Nature* **262**, 54–55.
- Thomas RC (1977). The role of bicarbonate, chloride and sodium ions in the regulation of intracellular pH in snail neurones. *J Physiol* **273**, 317–338.

- Uehlein N, Lovisollo C, Siefritz F & Kaldenhoff R (2003). The tobacco aquaporin NtAQP1 is a membrane CO₂ pore with physiological functions. *Nature* **425**, 734–737.
- Vallon V, Verkman AS & Schnermann J (2000). Luminal hypotonicity in proximal tubules of aquaporin-1-knockout mice. *Am J Physiol Renal Physiol* **278**, F1030–F1033.
- Vaughan-Jones RD (1982). Chloride activity and its control in skeletal and cardiac muscle. *Philos Trans R Soc Lond B Biol Sci* **299**, 537–548.
- Vaughan-Jones RD, Spitzer KW & Swietach P (2009). Intracellular pH regulation in heart. *J Mol Cell Cardiol* **46**, 318–331.
- Verlander JW, Miller RT, Frank AE, Royaux IE, Kim YH & Weiner ID (2003). Localization of the ammonium transporter proteins RhBG and RhCG in mouse kidney. *Am J Physiol Renal Physiol* **284**, F323–F337.
- Waisbren SJ, Geibel JP, Boron WF & Modlin IM (1994a). Luminal perfusion of isolated gastric glands. *Am J Physiol Cell Physiol* **266**, C1013–C1027.
- Waisbren SJ, Geibel JP, Modlin IM & Boron WF (1994b). Unusual permeability properties of gastric gland cells. *Nature* **368**, 332–335.
- Walter A & Gutknecht J (1986). Permeability of small nonelectrolytes through lipid bilayer membranes. *J Membr Biol* **90**, 207–217.
- Wang Y, Cohen J, Boron WF, Schulten K & Tajkhorshid E (2007). Exploring gas permeability of cellular membranes and membrane channels with molecular dynamics. *J Struct Biol* **157**, 534–544.
- Warburg O (1910). Über die oxydationen in lebenden Zellen nach Versuchen am Seeigeelei. *Hoppe-Seyler's Z Physiol Chem* **66**, 305–340.
- Weast RC (1978). *Handbook of Chemistry and Physics*. CRC Press, West Palm Beach, FL.
- Weiner ID (2006). Expression of the non-erythroid Rh glycoproteins in mammalian tissues. *Transfus Clin Biol* **13**, 159–163.
- Weiner ID & Verlander JW (2003). Renal and hepatic expression of the ammonium transporter proteins, Rh B Glycoprotein and Rh C Glycoprotein. *Acta Physiol Scand* **179**, 331–338.
- Weiner ID & Verlander JW (2010). Molecular physiology of the Rh ammonia transport proteins. *Curr Opin Nephrol Hypertens* **19**, 471–477.
- Xu L, Courtney NA, Radford TS & Boron WF (2010). Effect of AQP1 knock out on mouse exercise tolerance. *FASEB J* **24**, 1024.7.
- Yang B, Fukuda N, Van Hoek A, Matthay MA, Ma T & Verkman AS (2000). Carbon dioxide permeability of aquaporin-1 measured in erythrocytes and lung of aquaporin-1 null mice and in reconstituted liposomes. *J Biol Chem* **275**, 2686–2692.
- Zhao J, Hogan EM, Bevensee MO & Boron WF (1995). Out-of-equilibrium CO₂/HCO₃⁻ solutions and their use in characterizing a new K/HCO₃ cotransporter. *Nature* **374**, 636–639.
- Zheng L, Kostrewa D, Berneche S, Winkler FK & Li XD (2004). The mechanism of ammonia transport based on the crystal structure of AmtB of *Escherichia coli*. *Proc Natl Acad Sci USA* **101**, 17090–17095.
- Zhou Y, Bouyer P & Boron WF (2006). Evidence that AQP1 is a functional CO₂ channel in proximal tubules. *FASEB J* **20**, A1225.

Acknowledgements

I thank Drs Raif Musa-Aziz, Carlos Obejero-Paz, Mark Parker and Emad Tajkhorshid for helpful comments. The writing of this review was supported by Office of Naval Research grant N00014-08-1-0532.